SOURCES AND REMEDIES OF HIGH-FREQUENCY PIPING VIBRATION AND NOISE

by
Stephen M. Price
Senior Project Engineer
and
Donald R. Smith
Senior Staff Engineer
Engineering Dynamics Inc.
San Antonio, Texas

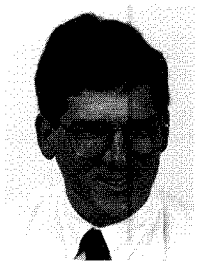

Stephen M. Price is a Senior Project Engineer for Engineering Dynamics Inc., in San Antonio, Texas. For the past 15 years, he has been actively involved in solving a variety of problems in systems that have experienced failures due to dynamic phenomenon. He has had field and analytical experience solving problems with reciprocating and rotating machinery, along with structural and acoustical problems. Additionally, Mr. Price has been involved in development of multiple channel data acquisition and monitoring hardware and software for critical environments. He has presented and published several papers in the areas of signal processing, finite element analysis, fatigue analysis, acoustics, and reciprocating pumps.

Mr. Price has a B.S. degree (Mechanical Engineering) from Mississippi State University and an M.S. degree (Mechanical Engineering) from Purdue University. He is a registered Professional Engineer in the State of Texas and a member of ASME.

Donald R. Smith is a Senior Staff Engineer at Engineering Dynamics Inc. (EDI), in San Antonio, Texas. For the past 30 years, he has been active in the field engineering services, specializing in the analysis of vibration, pulsation, and noise problems with rotating and reciprocating equipment. He has authored and presented several technical papers. Prior to joining EDI, he worked at Southwest Research Institute for 15 years as a Senior Research Scientist, where he was also involved in troubleshooting and failure analysis of piping and machinery.

Mr. Smith received his B.S. degree (Physics, 1969) from Trinity University. He is a member of ASME and the Vibration Institute.

ABSTRACT

In large diameter piping, high-frequency energy can produce excessive noise and vibration, and failures of thermowells, instrumentation, and attached small-bore piping. In severe cases, the pipe itself can fracture. Perhaps more precisely called "high wave number" problems, these problems most often manifest themselves in centrifugal compressors, screw compressors, heat exchangers, and silencers.

Two high-frequency energy generation mechanisms predominate in most industrial processes; flow induced (vortex shedding) and pulsation at multiples of running speed (blade-pass in centrifugal compressors and pocket-passing frequency in screw compressors). Once this energy is generated, amplification may occur from acoustical and/or structural resonances, resulting in high amplitude vibration and noise.

To resolve these problems successfully, an understanding of the underlying physics of two- and three-dimensional acoustics is necessary. With these principles in mind, modifications to the piping system can be considered for the particular application. The three-dimensional wave equation is used to analyze the propagation of the high-order (cross-wall) acoustical modes in the duct or pipe. These cross-wall modes can be diametrical (m) modes, annular (n) modes, or combined (m, n) modes. By reformulating the resulting differential equations into polar coordinates and applying the appropriate boundary conditions, an equation for the "cut-on" frequencies, $f_{(m,n)}$, for cross-wall modes can be developed that incorporates zeroes of the first order Bessel function, $\beta_{(m,n)}$, the speed of sound, and pipe diameter. Several references provide lists of the zeroes of the Bessel function; however, most of these references only provide solutions up to m, n = 6. Field tests have identified cross-wall modes up to m = 30. Therefore, a table is provided for zeros of $\beta_{(m,n)}$ for m = 0 to 32 and n = 0 to 8.

This paper discusses the excitation and amplification mechanisms relevant to high-frequency energy generation in piping systems. Mechanisms that allow efficient coupling of this energy with the surroundings (either structural or acoustical) are discussed. Data from various systems are presented, as well as design modifications that have been shown to be effective at reducing the high-frequency energy.

EXCITATION MECHANISMS

The main sources of the high-frequency pulsation are usually vortex shedding and/or blade-pass excitation. The high-frequency pulsation typically occurs at frequencies above approximately 500 Hz, although for systems with large diameter vessels, such problems can exist at lower frequencies. Vortex shedding is a phenomenon that occurs due to flow over an obstruction. In turbomachinery, the primary excitation is due to the interaction of a blade or vane with the internal passages. Pulsation occurs at the blade-pass frequency (number of blades multiplied by the operating speed) and multiples of blade-pass frequency. In screw compressors, the intermeshing of the helical lobes generate pulsation at the pocket-passing frequency (the number of lobes on the male rotor multiplied by the running speed) and multiples of the pocket-passing frequency.

Vortex Shedding

Vortex shedding occurs due to flow over an obstruction in the flow path. At low flow velocities (low Reynolds number), a fluid particle can flow completely around the obstruction. However at

higher Reynolds numbers, the fluid boundary layer at the trailing edge of the obstruction will separate, causing shear layers that trail the obstruction. These shear layers tend to roll into vortices that are alternately shed from either side of the obstruction (Figure 1). The alternate shedding occurs at regular intervals and therefore produces an oscillating pressure field (pulsation).

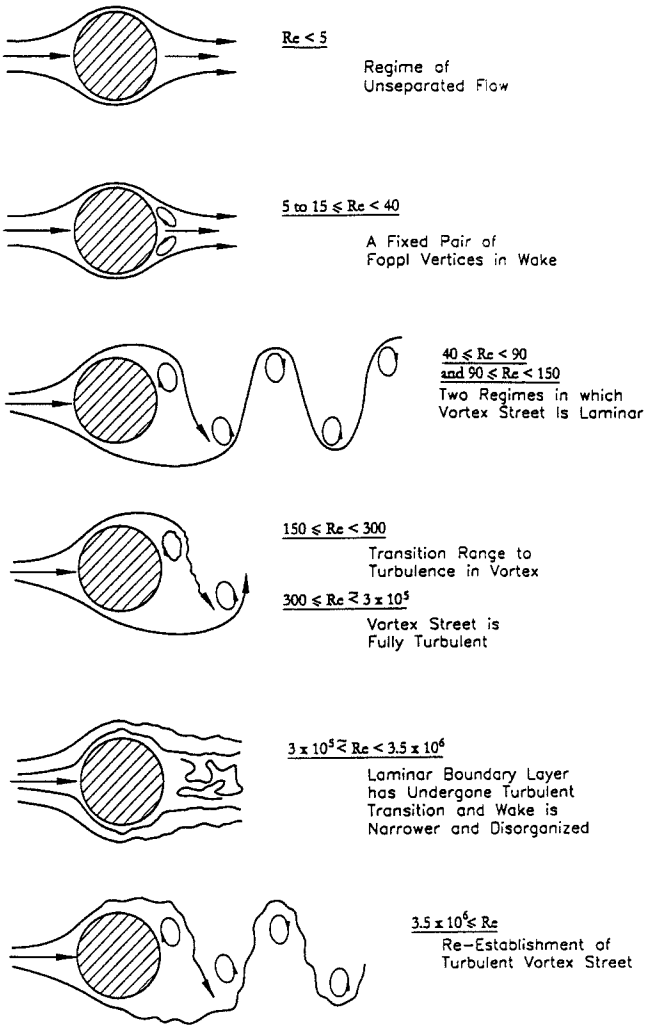

Figure 1. Vortex Shedding Across an Obstruction for Different Flow Regimes.

Pulsation induced by vortex shedding can be extremely complex. A detailed explanation of this phenomenon is available in Blevins (1973). However, a simplified analysis can be performed using the concept of the Strouhal number. The frequency of the vortex shedding can be described by Equation (1):

$$f = \frac{SV}{D} \tag{1}$$

where:

f = Vortex shedding frequency, Hz
V = Flow velocity, ft/sec
S = Strouhal number
D = Effective diameter of the obstruction (ft)

Note that the vortex shedding frequency *f* increases with increasing flow velocity *V*. For a single smooth tube, the vortex shedding Strouhal number is approximately 0.2. When several tubes are grouped together (as in a heat exchanger or boiler), the Strouhal number can range from 0.2 to 1.0. It has been found that the Strouhal number for flow across obstructions typically ranges from 0.2 to 0.5.

Blade-Pass/Pocket-Pass Excitation

In centrifugal compressors, energy can be created by the action of the blades passing by various internal components of the compressor. As a blade tip moves past some internal clearance, a wake is generated that produces a pressure pulse. This action is termed blade-pass excitation. In screw compressors, the intermeshing of the helical lobes of the male and female rotors create progressive cavities that produce flow modulations in the inlet as the cavity is formed, and in the outlet as the cavity discharges its contents.

The frequency of this energy (f_{bp}) is the running speed multiplied by the number of blades on the impeller wheel (for centrifugal compressors), or the number of lobes on the male rotor multiplied by compressor running speed (for screw compressors). Energy can also occur at integer multiples of blade-pass or pocket-pass frequencies.

$$f_{bp} = i(n)\ (rpm) \tag{2}$$

where:

f_{bp} = Pulsation frequency, cpm
i = 1, 2, 3...
n = Number of impeller vanes (blades) or lobes on the male rotor
rpm = Compressor speed

Depending upon the internal geometry of the compressor, other "passing" frequencies may be generated between the blades and the inlet guide vanes, diffusers, etc.

AMPLIFICATION MECHANISMS

The high-frequency energy generation mechanisms discussed above generally produce very low pulsation amplitudes (0.5 psi peak-to-peak or less). Alone, this energy is not usually sufficient to cause significant vibration or noise. However, just as a radio receiver amplifies minute electromagnetic variations into audible sound, various amplification mechanisms exist that can amplify low-level energy to annoying or dangerous levels.

Acoustic Cross-Wall Natural Frequencies

Pulsation in reciprocating compressors and positive displacement pumps can generally be described using one-dimensional acoustics. In one-dimensional acoustics, the wavelength of the pulsation is long compared with the pipe diameter, and the pressure pulse travels as a plane wave. In a one-dimensional model, the pressure (and flow) properties are assumed to vary only along the length of the pipe and are constant over the cross-sectional area.

However, in large diameter ducts and piping, the wavelengths of the waves that propagate can be shorter than the characteristic dimension of the duct or pipe. When this occurs, the wave propagates at an oblique angle relative to the duct or pipe wall, as compared with the plane wave propagation in which the direction of propagation is parallel to the duct wall. As a result, wave interference patterns called cross-wall modes are formed in the duct or pipe. The acoustic pressure across a specific duct cross-section is not constant, but varies as a function of the distance across the duct. These acoustical natural frequencies are sometimes referred to as cross-wall or high-order modes.

The three-dimensional wave equation is used to analyze the propagation of the cross-wall modes in the duct or pipe. The differential equations can be simplified by reformulating the equation into polar coordinates and applying the appropriate boundary conditions (particle displacement is zero at the pipe walls, etc.) and assuming a solution in the form of a Bessel function. The piping cross-wall acoustic natural frequencies can be computed using Equation (3):

$$F_{(m,n)} = \frac{\beta_{(m,n)} c}{\pi d} \quad (3)$$

where:

$F_{(m,n)}$ = Pulsation frequency, Hz
$\beta_{(m,n)}$ = Zeros of the first order Bessel function
c = Speed of sound, ft/sec
d = Pipe diameter, ft

The first order Bessel function is a continuous function that is roughly sinusoidal in shape. Values for the zero crossings of this function are shown in Figure 2. The modes are designated by ordered pair (m, n) where the integer "m" determines the number of radial (diametrical) nodal lines, and the integer "n" determines the number of the annular (circumferential) nodal circles.

m↓ n→	0	1	2	3	4	5	6	7	8
0	0.00	3.83	7.02	10.17	13.32	16.47	19.62	22.76	25.90
1	1.84	5.33	8.54	11.71	14.86	18.02	21.16	24.31	27.46
2	3.05	6.71	9.97	13.17	16.35	19.51	22.67	25.83	28.98
3	4.20	8.02	11.35	14.59	17.79	20.97	24.14	27.31	30.47
4	5.32	9.28	12.68	15.96	19.20	22.40	25.59	28.77	31.94
5	6.42	10.52	13.99	17.31	20.58	23.80	27.01	30.20	33.39
6	7.50	11.73	15.27	18.64	21.93	25.18	28.41	31.62	34.81
7	8.58	12.93	16.53	19.94	23.27	26.55	29.79	33.02	36.22
8	9.65	14.12	17.77	21.23	24.59	27.89	31.16	34.40	37.62
9	10.71	15.29	19.00	22.50	25.89	29.22	32.51	35.76	39.00
10	11.77	16.45	20.22	23.76	27.18	30.53	33.84	37.12	40.37
11	12.83	17.60	21.43	25.01	28.46	31.84	35.17	38.46	41.73
12	13.88	18.75	22.63	26.25	29.73	33.13	36.48	39.79	43.08
13	14.93	19.88	23.82	27.47	30.99	34.41	37.78	41.11	44.41
14	15.98	21.02	25.00	28.69	32.24	35.69	39.08	42.43	45.74
15	17.02	22.14	26.18	29.91	33.48	36.95	40.37	43.73	47.06
16	18.06	23.26	27.35	31.11	34.71	38.21	41.64	45.03	48.37
17	19.10	24.38	28.51	32.31	35.94	39.46	42.91	46.31	49.67
18	20.14	25.50	29.67	33.50	37.16	40.71	44.18	47.60	50.97
19	21.18	26.61	30.82	34.69	38.38	41.94	45.44	48.87	52.26
20	22.22	27.71	31.97	35.87	39.58	43.18	46.69	50.14	53.55
21	23.25	28.82	33.12	37.05	40.79	44.40	47.93	51.40	54.82
22	24.29	29.92	34.26	38.22	41.99	45.62	49.17	52.66	56.10
23	25.32	31.01	35.40	39.39	43.18	46.84	50.41	53.91	57.36
24	26.36	32.11	36.53	40.56	44.37	48.05	51.64	55.16	58.62
25	27.39	33.20	37.66	41.72	45.56	49.26	52.87	56.40	59.88
26	28.42	34.29	38.79	42.88	46.74	50.46	54.09	57.64	61.13
27	29.45	35.38	39.92	44.03	47.92	51.66	55.30	58.87	62.38
28	30.48	36.47	41.04	45.18	49.10	52.86	56.52	60.10	63.63
29	31.51	37.55	42.16	46.33	50.27	54.05	57.73	61.33	64.87
30	32.53	38.64	43.28	47.48	51.44	55.24	58.93	62.55	66.10
31	33.56	39.72	44.40	48.62	52.60	56.42	60.14	63.77	67.33
32	34.59	40.80	45.51	49.76	53.77	57.61	61.34	64.98	68.56

Figure 2. Zeros of First Order Bessel Function.

Figure 3 shows a representation of the pressure mode shapes for diametrical modes m = 1 to 4, n = 0, and for annular modes m = 0, n = 1 to 4. The mixed modes (where both m and n are nonzero) are not shown because of their complexity. In all cases, there is a pressure maximum at the wall of the pipe and pressure minima along the nodal lines shown in the diagrams.

Previous laboratory testing has determined that the diametrical modes ("m" modes) are easily excited when the excitation source is near the pipe wall. Similarly, the circumferential modes ("n" modes) are easily excited when the excitation source is near the center of the piping (along the axis of the pipe).

The cross-wall acoustic natural frequencies are also referred to as cut-on, or cutoff frequencies. Below the first cross-wall natural frequency, m = 1, n = 0 (cutoff frequency), only plane wave propagation is possible. However, at frequencies above the first cross-wall natural frequency (cut-on frequency), the two-dimensional cross-wall modes can propagate down the piping. Furthermore, above the cut-on frequency, these modes have little or no damping and can travel long distances unattenuated.

Shell Wall Natural Frequencies

At low frequencies, pipe vibration occurs laterally along its length (like a beam). At higher frequencies, the pipe shell wall

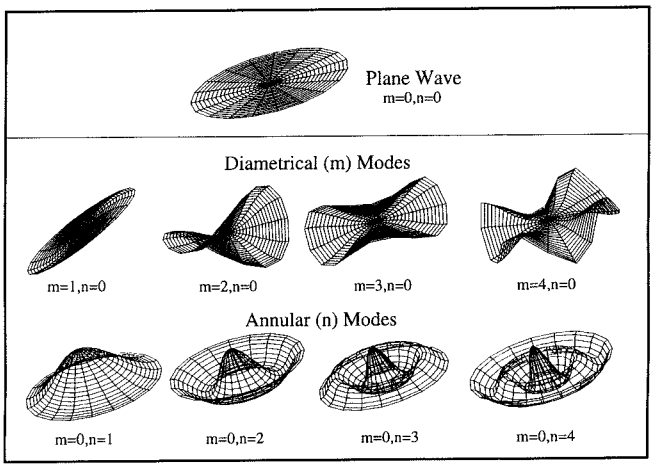

Figure 3. Cross-Wall Acoustical Mode Shapes for (m = 1 to 4, n = 0) and (m = 0, n = 1 to 4).

begins to vibrate radially across its cross-section. This could be viewed as a "breathing" mode if all points were vibrating in-phase. At progressively higher frequencies, adjacent portions of the pipe shell may vibrate out-of-phase, producing a sine-wave around the circumference. Examples of these mode shapes are shown in Figure 4.

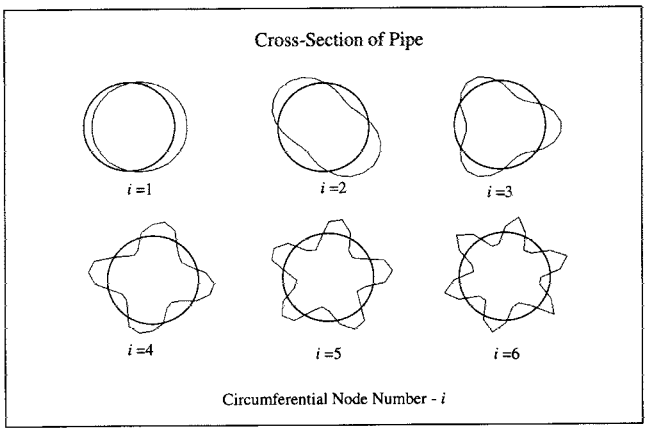

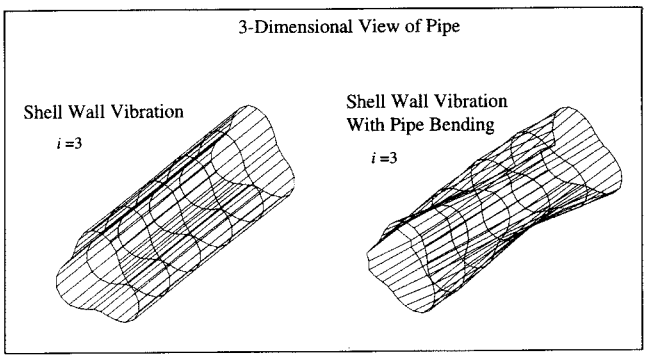

Figure 4. Piping Shell Wall Vibration Mode Shapes.

A number of theories can be used to calculate the shell wall natural frequencies for shell wall vibration. For infinitely long pipe, a closed form solution has been developed, as provided in Blevins (1979). Using Equation (4) and Equation (5), it can be shown that the natural frequencies are primarily controlled by the piping diameter and wall thickness. The frequencies are also slightly influenced by the internal pressure in the piping. To account for internal pressure, the effective pipe wall thickness should increase by 5 percent to 10 percent.

Experience has shown that the accuracy of these calculations is sufficient for a pipe span approximately one diameter away from significant discontinuities (e.g., flanges, tees, elbows, etc.).

$$f_i = \frac{\lambda_i}{2\pi R}\left[\frac{E}{\gamma(1-\nu^2)}\right]^{1/2} \quad (4)$$

$$\lambda_i = \frac{1}{12^{1/2}}\frac{h}{R}\frac{i(i^2-1)}{(1+i^2)^{1/2}} \quad (5)$$

where:

fi = Shell wall natural frequency, Hz
λi = Frequency factor, dimensionless
R = Mean radius of pipe wall, inch
ν = Poisson's ratio
γ = Mass density of pipe material, lb/g-in^3
E = Modulus of elasticity of pipe wall, psi
h = Pipe wall thickness, inch
i = Mode number, 2, 3, 4...
g = Gravitational constant, inch/sec^2

Radiation Efficiency

Each of these shell wall natural frequencies (f_i, i = 2, 3, 4...) has a particular mode shape defined by the number of diametrical node lines (Figure 4). For a particular mode shape to be an efficient radiator of noise (or conversely, to be easily excited by pulsation), the bending wavelength of the shell wall vibration must be equal to or greater than the wavelength of the acoustical wave in air. This characteristic is termed radiation efficiency.

The point at which the two wavelengths match is called the coincidence frequency. If the shell wall natural frequency is lower than the coincidence frequency, the mode will not be an efficient radiator of noise. At shell wall frequencies above the coincidence frequency, the mode can radiate sound effectively.

The coincidence frequency is defined by Equation (6).

$$f_c = \frac{c_{air}}{\lambda_b} \quad (6)$$

where c_{air} is the speed of sound in air and λ_b is the bending wavelength of the shell wall mode. For pipes, the shell wall modes have a bending wavelength defined by:

$$\lambda_b = \frac{\pi d}{N} \quad (7)$$

where d is the diameter of the pipe and N is the number of diametrical node lines.

The evaluation of whether a mode is an efficient radiator of sound is made simpler by computing the ratio of its natural frequency, f_i, to the coincidence frequency, f_c. Modes that have ratios greater than or approximately equal to 1.0 will radiate sound. Values less than approximately 0.7 denote modes that are poor radiators of sound.

The radiation efficiency concept also provides an indication of the degree of coupling between pulsation in the gas inside the pipe, to shell wall vibration.

$$f_c = \frac{c_{gas}}{\lambda_b} \quad (8)$$

where c_{gas} is the speed of sound in the gas. Values greater than one will denote modes that can transfer energy to the pipe wall easily, while values less than one denote modes that are less efficient at transferring their energy.

Equation (4) through Equation (8) can easily be set up into a spreadsheet for computation. One such computation for a heavy hydrocarbon flowing in a 36 inch steel pipe is shown in the table in the section, *Calculations*.

REDUCING HIGH-FREQUENCY PULSATION AND VIBRATION

There are several techniques available to achieve reductions of high-frequency energy. The energy generation mechanisms can be reduced or eliminated, and/or the amplification mechanisms can be removed. Additionally, it is sometimes possible to simply control the vibration by using damping, or to reduce the pulsation energy by using acoustical absorption material inside the pipe.

Reduction of Vortex Shedding Energy

The first step to reducing vortex shedding energy (pulsation) is to identify the particular components causing shedding. Since the frequency of the excitation is known, Equation (1) can be used to determine the approximate size of the obstruction. With this information, it should be possible to determine if an obstruction (or gap) exists in the piping that conforms to the required size that would result in pulsation in the frequency range of interest.

Sometimes, these structures can be modified to discourage shedding, or to change the shedding frequencies. Figure 5 shows several ways to reduce vortex shedding. Adding strakes or airfoil shapes are the most commonly used methods.

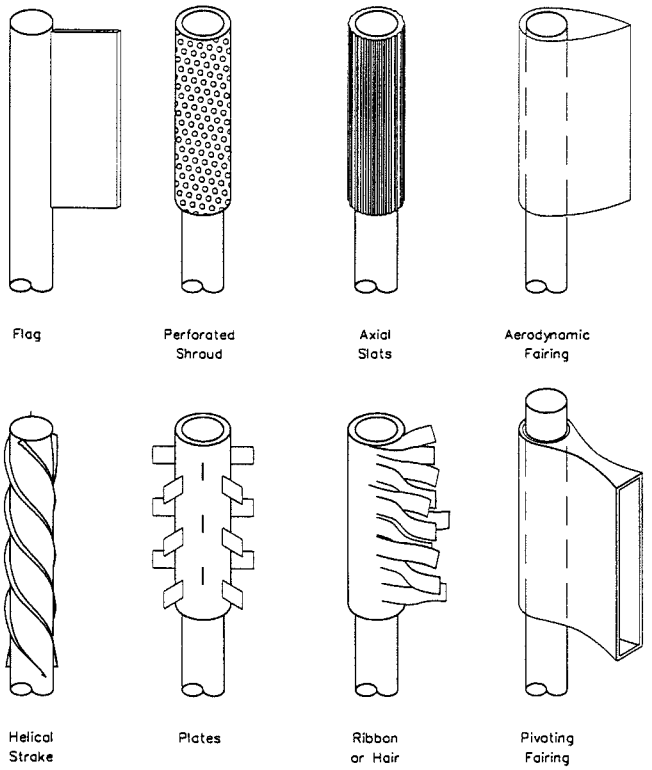

Figure 5. Vortex Suppression Devices.

If prevention of vortex shedding is not practical, the vortex shedding frequencies can be shifted away from acoustical or mechanical natural frequencies by making the effective diameter of the obstruction larger or smaller. Alternatively, the flow path could be altered to reduce or increase velocities across the obstruction.

Reduction of Blade-Pass Pulsation

Since blade-pass pulsation is caused by interactions within the compressor, it is usually difficult to reduce blade-pass excitation without altering compressor performance. The compressor manufacturer should be consulted to assess possible methods to

reduce blade-pass energy. Increasing the internal clearances between the impeller vanes and diffuser blades or cutwater ("B Gap," Figure 6) has been shown to be effective in some cases. Modification of the flow-path has also been successful.

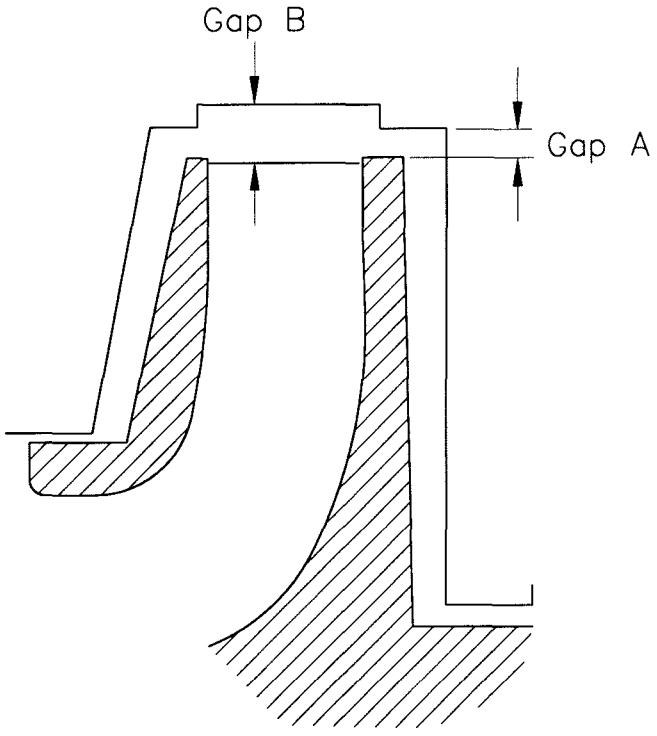

Figure 6. Cutwater ("B" Gap) Clearance.

If it is not possible to reduce blade-pass energy amplitudes, changing the number of impeller blades can shift the frequency. Adding blades generally produces lower amplitude blade-pass energy.

Prevention of Cross-Wall Acoustical Modes

Changing the internal dimensions of the pipe can shift the natural frequencies of cross-wall modes. However, since it is not usually practical to provide a significant diameter change, "flow-splitters" can be added inside the pipe to change the internal geometry, which significantly shifts the cross-wall natural frequencies.

Depending upon the frequencies and number of modes involved, an internal X-brace (Figure 7) may be sufficient. In some cases, a more complicated modification called a "tube bundle" may be required (Figure 7). A potential problem with such modifications is that the cross-wall modes can re-form in the piping upstream or downstream of the tube bundle or X-brace. It is difficult to determine the length of the tube bundle or X-brace required to prevent reformation of the cross-wall modes. Laboratory tests indicated that for tube bundles that are several pipe diameters in length, the cross-wall modes tend not to re-form, but for flow splitters, the modes may re-form downstream of the splitter.

Another method to attenuate cross-wall modes is with acoustically absorptive material (Figure 8). Since all the cross-wall modes have a maximum pressure boundary at the edge of the pipe, applying absorption material at this boundary (which enforces a pressure-release condition) will discourage cross-wall mode formation. One drawback to this approach is that absorption material inside the pipe is not acceptable under many circumstances (e.g., when liquids are present, high temperatures, etc.). Also, it can be difficult to contain the absorption material. Often, the absorption material is restrained with wire mesh or perforated metal.

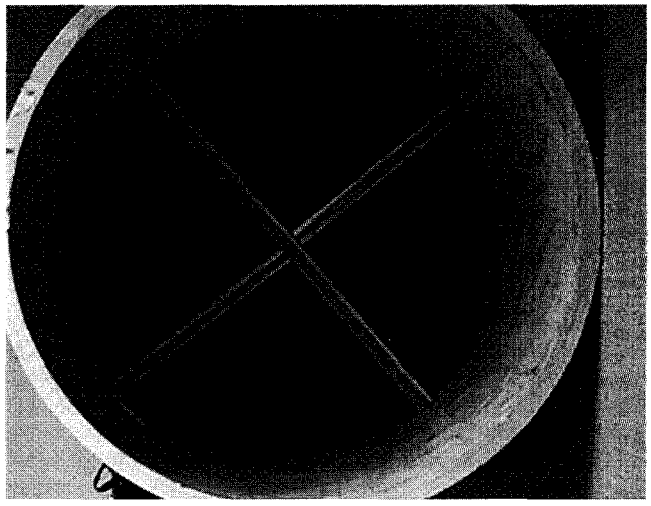

X-Brace in Pipe

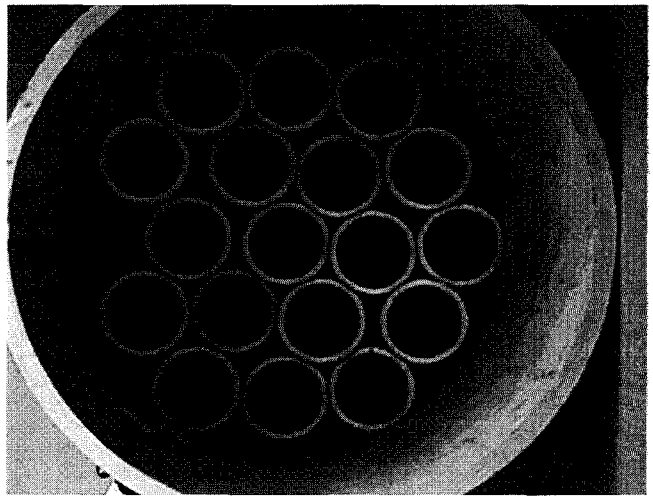

Tube Bundle in Pipe

Figure 7. Internal Pipe Modification to Discourage Acoustic Cross-Wall Mode Formation.

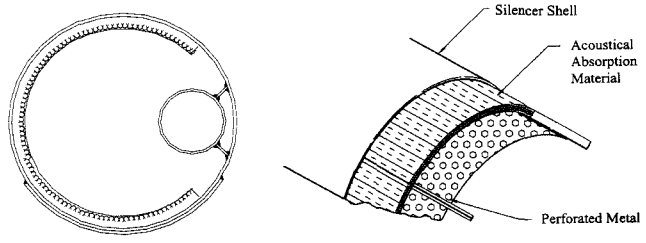

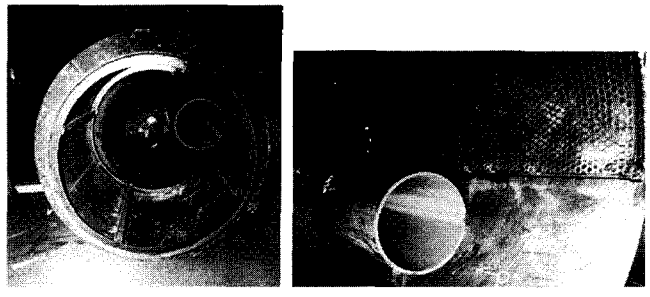

Figure 8. Absorption Material Applied to Silencer Internals.

A final method to dissipate high-frequency energy is through use of reactive silencers. These silencers make use of various volume and choke tube arrangements to attenuate the energy before it can propagate into the piping. However, care must be taken to design the silencer so that cross-wall modes do not form in the silencer itself. A poorly designed "silencer" can actually become an amplifier, potentially creating destructive levels of pulsation and vibration energy. Additionally, the silencer internals can be prone to vibration induced failures.

Reduction of Shell Wall Vibration

In some cases, it is not practical to reduce the pulsation energy sources or attenuate the acoustical cross-wall modes. Increasing the pipe wall thickness can reduce the shell vibration levels. However, it is generally impractical to replace existing piping with thicker wall piping. In these cases, adding damping to the piping and surrounding structures can be effective at reducing the shell vibration amplitudes. There are two basic types of damping treatment for structural damping: extensional (unconstrained or free-layer damping) and shear (constrained-layer damping).

Extensional damping treatment (Figure 9) consists of a single piece of visco-elastic damping material bonded directly to the structure surface. As the surface deforms, the damping material is subjected to tension-compression deformation. While this type of damping is the easiest to design and apply, extensional damping is usually not as effective as constrained-layer damping.

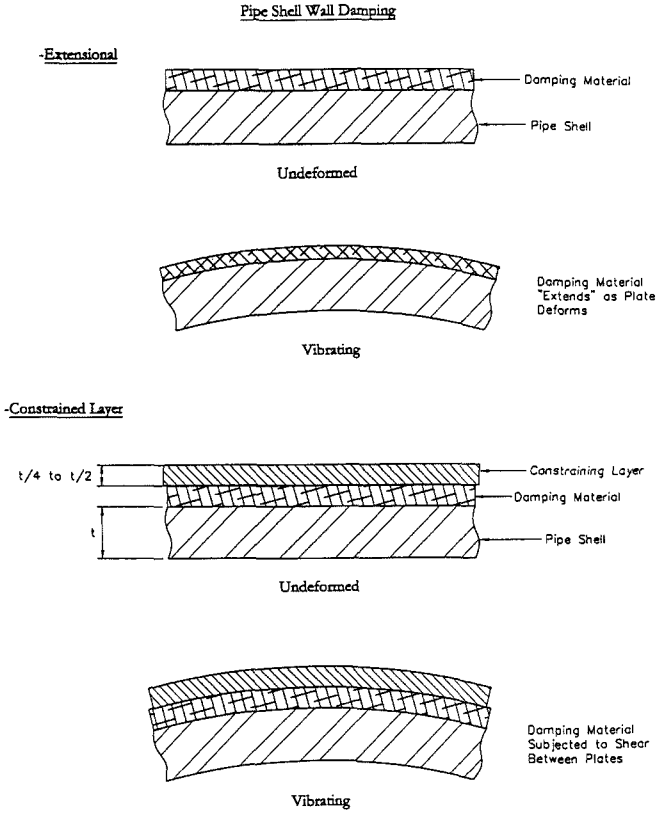

Figure 9. Plate and Shell Damping Treatments—Extensional and Constrained Layer.

Constrained-layer damping (Figure 9) is similar to extensional damping, except that the damping material is constrained by an outer metal layer. As the pipe wall is deformed, the outer metal layer constrains the damping material and forces it to deform in shear. The thickness of the outer metal layer and the thickness and material properties of the damping material control the effectiveness of the constrained-layer damping. Normally, the thickness of the outer metal layer should be approximately 25 percent to 50 percent of the pipe wall thickness. Theoretically, the maximum damping is obtained with very thin damping material, since the shear is higher.

For flat plates, a very thin damping layer can be used. However, for large diameter piping, it can be impractical to fabricate a constraining layer with tolerances less than one-eighth inch. Thicker damping material can be used (good success has been had using sheets of silicone rubber or neoprene), but the effective damping will be reduced from the ideal case.

Acoustical Lagging

For situations where vibration is not a problem, but noise levels are excessive, it is sometimes desirable to add acoustical "lagging" to the piping to absorb the noise, rather than to try to reduce the source or amplification mechanisms. The choice of lagging material is important. Absorption material that is appropriate for the frequency of noise must be selected.

A typical lagging application is shown in Figure 10 (adapted from Pelton, 1993). Note that the absorption material is surrounded by a mass layer (usually lead or vinyl). Lower frequency applications will require thicker mass layers. In some cases, several sandwiches of absorption material, mass layer, must be used to achieve acceptable noise attenuation.

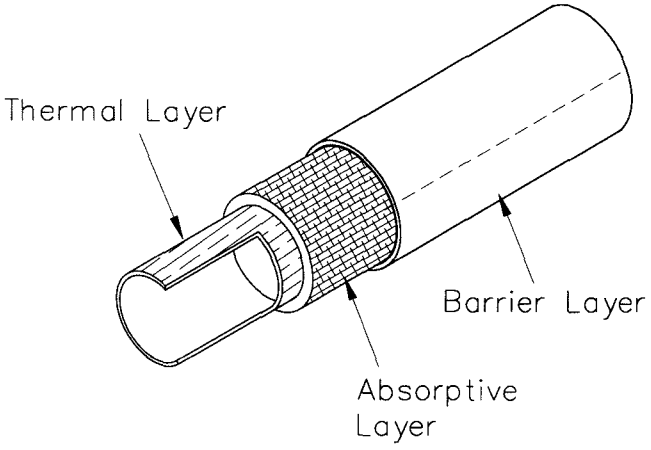

Figure 10. Acoustical Lagging Applied to the Exterior of a Pipe.

TESTING

To diagnose these types of problems, field testing is usually required. The test program philosophy is to try to identify energy generation mechanisms (such as blade-pass pulsation or vortex shedding) and determine transmission paths and/or amplification mechanisms. Eliminating energy generation, short-circuiting the transmission path, and/or changing the amplification mechanisms can reduce vibration and noise. The following sections describe a typical instrumentation and test procedure.

Instrumentation

A variety of instrumentation is required, including high-frequency accelerometers, insertion pulsation probes, microphones, strain gauges, and impact hammers.

High-Frequency Accelerometers

Measurement of piping shell wall vibration requires low-mass, high-frequency accelerometers. The accelerometers should be attached to pads that are either glued or welded onto the structure. In some cases, acceleration levels in excess of 500 g's zero-peak have been measured. Such extreme amplitudes can damage accelerometers, or cause the electrical connections and wires to fail. Therefore, specially constructed wiring and accelerometers may be required.

Insertion Probes

Pulsation data should be acquired in the piping, especially near locations of high vibration and noise. Pulsation data are most often measured at "stubs" (i.e., through a valve or other connection). Such an installation will not provide an accurate indication of pulsation in the piping due to quarter-wave resonances. For a simple stub, these resonances will produce false peaks in the pulsation data at intervals and frequencies given by:

$$f_n = \frac{nc}{4L} \tag{9}$$

where:

f_n = Stub frequencies, Hz
n = 1, 3, 5...
c = Acoustic velocity, ft/sec
L = Length of stub, ft

In the field, such simple stub connections are rarely encountered. As shown in Figures 11 and 12, the stub piping typically consists of a number of diameter changes. These diameter changes cause impedance discontinuities, which result in multiple pulsation responses, rather than a single frequency.

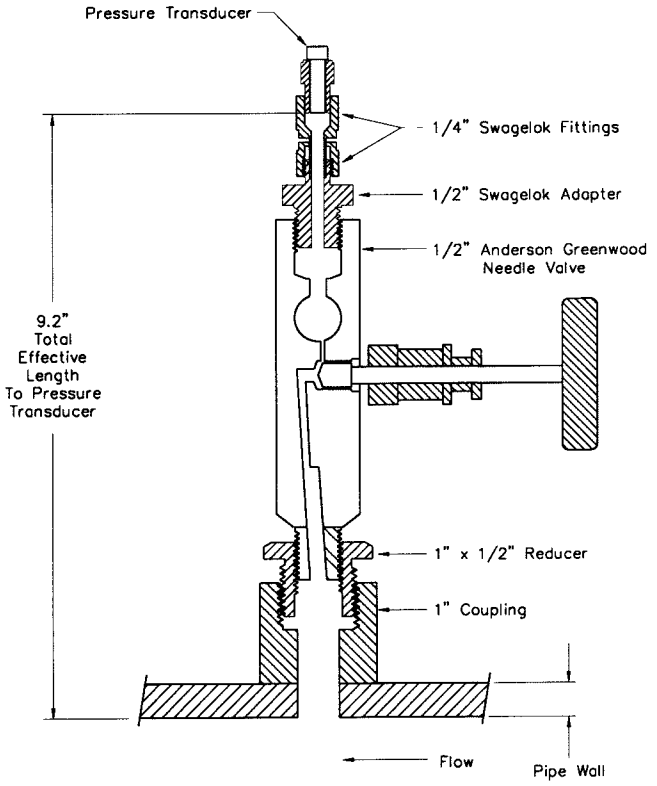

Figure 11. Pressure Transducer Stub Connection Through Needle Valve.

Additionally, as described in Kinsler, et al. (1982), the amplitude of pulsation can be higher, even at frequencies that are away from stub resonances, due to the effects of pressure reflection at a closed end. Therefore, to avoid these potential problems, it is desirable to position the pulsation transducer just inside the shell wall of the piping.

In many cases, it is also desirable to install and remove the pressure transducer without depressurizing the system. One company has developed an "insertion probe" that allows the pressure transducer to be inserted through a valve, and positioned inside the pipe wall (Figure 13). This arrangement has been installed successfully into operating systems with pressures as high as 2500 psi.

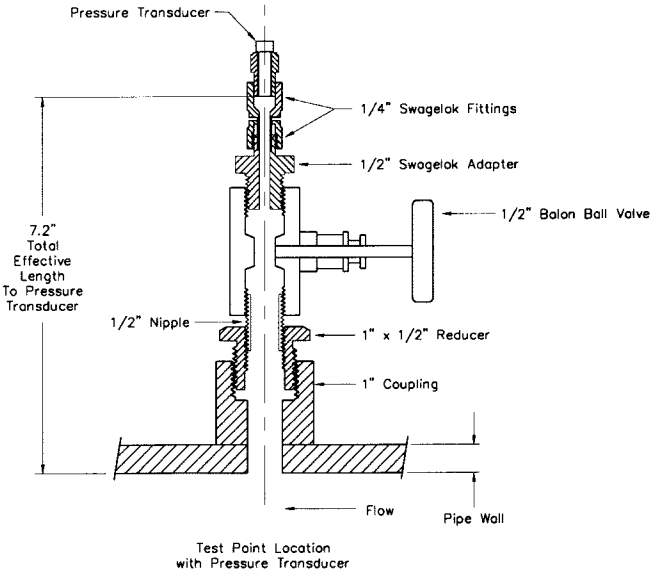

Figure 12. Pressure Transducer Stub Connection Through Ball Valve.

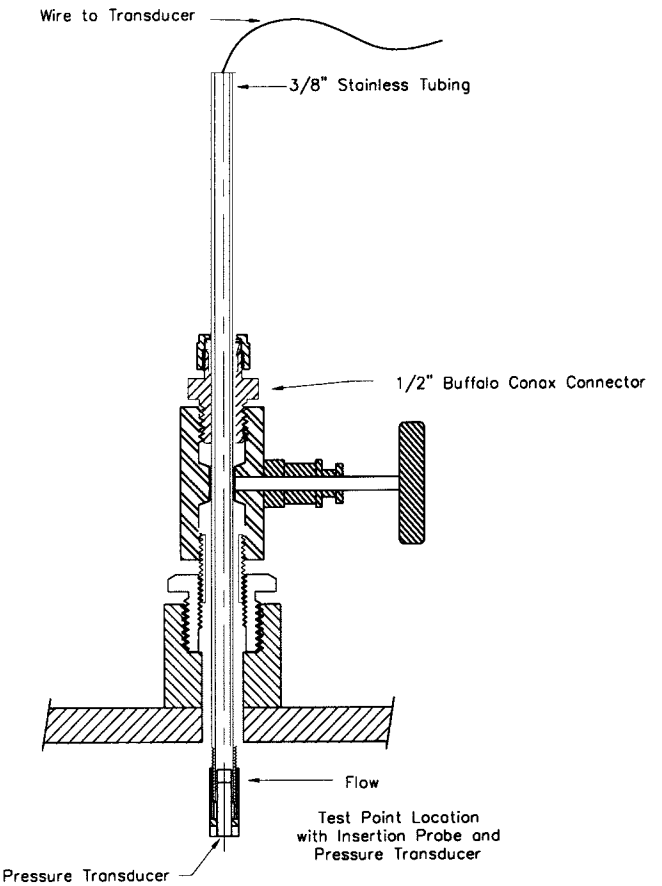

Figure 13. Insertion Probe to Eliminate Stub Connection.

Microphones

Sound data are used to correlate ambient noise with piping vibration and pulsation. Several microphones positioned a few feet from the piping shell will produce data that allow such comparisons to be made. It has been found that in most cases, inexpensive self-contained sound-level meters provide adequate data for these purposes.

Strain Gauges

Strain gauges are used to determine strain levels in the piping and at nozzle connections. Weldable gauges provide the largest range of operating conditions, and are easy to install. However, a small spot welder is required to attach these gauges. Using these gauges, comparisons of measured strain frequencies and amplitudes to the vibration, pulsation, and noise can be made to provide insight into the causes of failures.

Impact Hammers

Natural frequency testing of the piping shell walls can be accomplished easily with impact hammers. The hardness of the hammer tip should be selected to produce an impact having energy at the frequencies of interest. For example, if excitation at high-frequencies (>500 Hz) is desired, a steel tip should be used. For lower frequencies, plastic or rubber tips could be used. The mass of the hammer should also be selected so that the hammer rebounds quickly when the pipe is impacted. For most piping, the shell wall modes can be excited using a 1 lb hammer with a steel tip.

Test Procedure

A typical test procedure involves natural frequency testing of the system and operational tests.

Structural Natural Frequency Tests

Structural shell wall natural frequencies are amplification mechanisms that can result in high vibration when excited. These natural frequencies can be identified using an impact hammer and modal analysis software. Usually, it is necessary to shut down the system to obtain good quality natural frequency data. In addition to determining the natural frequency, the mode shape data are useful for determining the ability of a structural natural frequency to couple with pulsation or generate noise. To measure the mode shapes of the higher modes, data are acquired at several evenly spaced locations around the circumference of the pipe. The minimum number of test points required is twice the mode number (the number of diametrical node lines) for the highest frequency of interest. The mode shape for a particular natural frequency can be identified using these data and commercially available animated mode-shape software.

For example, consider a pipe with a 24 inch diameter and a 0.5 inch thick wall. Table 1 illustrates the number of circumferential test points required to define the mode shape. As shown, if the highest frequency of interest is 1500 Hz, at least 14 points around the circumference of the pipe would be required to define mode shapes for shell wall natural frequencies up to 1500 Hz.

Table 1. Minimum Number of Points Required to Define a Shell Wall Natural Frequency Mode Shape.

Mode #	Natural Frequency	# Points Required
2	95	4
3	368	6
4	513	8
5	830	10
6	1218	12
7	1677	14
8	2206	16

Operational Tests

After installing accelerometers, pressure transducers, strain gauges, and microphones, the system should be tested while operating at a variety of conditions. Note that in addition to the installed instrumentation, system parameters (e.g., pressures, temperatures, speed, etc.) should be logged. A tape recorder or other data acquisition system is necessary to gather all data simultaneously.

If the machine speed can be varied, a test should be performed where the machine's speed is varied slowly from minimum to maximum speed. Another test could be done by varying the loading. Additional tests should be performed with abnormal conditions (recycle operation, near-surge conditions, etc.).

Evaluation of Data

Data can be plotted in many formats. A spectrum analyzer, a digital acquisition system, and software for generating high quality plots will simplify the process and enhance evaluation of data.

Using the pulsation data, the energy generation mechanisms can be identified. For example, if pulsation is measured only at blade-pass frequency, the machine itself is generating the pulsation. Nonsynchronous frequencies could be related to vortex shedding or other phenomena.

Pulsation data obtained during a speed sweep can be compared with calculations of cross-wall natural frequencies to determine if pulsation energy is being amplified by cross-wall acoustical modes in the piping. Similarly, shell wall vibration data obtained during a speed sweep combined with data from natural frequency tests will help determine if structural responses could be amplifying energy.

Strain and microphone data should be compared with the pulsation and vibration data to determine which of the measured energies are contributing to the fatigue failures or high noise levels. Once these comparisons are made, it should be possible to develop solutions to reduce the vibration, stress, and noise using the concepts discussed in the previous section, REDUCING HIGH-FREQUENCY PULSATION AND VIBRATION.

Acceptability of Shell Wall Vibration

For shell wall piping vibration, acceptability criteria must relate vibration amplitudes to stress. Such a relationship has been developed by Mikasinovic (1989) in which vibration velocity measured on a cylindrical shell wall is related to dynamic strain:

$$V = \frac{c\varepsilon}{2\pi} \tag{10}$$

where:

V = Vibration velocity, in/sec, zero-peak
c = Curve fit constant = 742,124 in/sec
ε = Dynamic strain, microstrain (in/in $\times 10^{-6}$)

This relationship assumes that the vibration measurements are zero-peak measurements and that several resonant modes are involved (so that the peak vibration velocity is approximately the same around the circumference and along the axial length of the piping between the constraints). Mikasinovic tested pipe diameters from 6 inch to 30 inch, wall thicknesses from 0.25 inch to 0.75 inch, and lengths from 12 ft to 42 ft with satisfactory results. Good correlation has been obtained between measured and calculated strain values for 30 inch pipe with wall thicknesses of 0.375 inch to 0.8 inch.

Using this formula, it would be possible to relate the vibration velocity to the fatigue endurance limit. Assuming an allowable endurance limit stress for carbon steel of 13,000 psi zero-peak, a safety factor of 1.3, and a stress concentration factor of five (at the heat-affected zone of a weld), the allowable stress would be 2000 psi zero-peak. For carbon steel, the elastic modulus is 30,000,000 psi, which results in an allowable strain of approximately 67 microstrain zero-peak (133 microstrain peak-to-peak). Using this value for the acceptable strain in Equation (10), the allowable velocity is 7.9 in/sec zero-peak.

If the stress concentration factor is less than the maximum, the allowable vibration velocity would be higher by the ratio of the actual stress concentration factor to five. For example, a butt weld has a stress concentration factor of approximately two; therefore, the allowable velocity would be increased to 19.8 psi zero-peak. This allowable vibration is considerably higher than the allowable levels for lateral piping vibration and machinery vibration (e.g., at a bearing housing).

The vibrational velocity of the shell wall can also be related to the sound pressure level (C or linear weighting). Field experience with strain gauges installed on piping with high-frequency, broadband, vibrations has shown that the sound pressure level (SPL) measured approximately 1 inch away from the pipe wall is proportional to the dynamic strain. Although the relationship between dynamic strain and SPL amplitude is not exact, the overall levels presented below have been used to estimate the severity of shell wall vibrations and as a screening method to help determine where strain gauges should be installed on a piping system.

When the SPL is measured with a sound level meter (SLM) using C weighting approximately 1 inch from the vibrating pipe wall, the following criteria have been found to be applicable:

- 130 dB is equivalent to approximately 100 microstrain peak-to-peak
- 136 dB is equivalent to approximately 200 microstrain peak-to-peak

In addition to the criteria outlined above, it has been shown by field experience that allowable strain levels (ε) for carbon steel can be specified by:

	$\varepsilon <$	100 microstrain p-p	Safe
100 microstrain p-p	$< \varepsilon <$	200 microstrain p-p	Marginal
	$\varepsilon >$	200 microstrain p-p	Excessive

Therefore, sound pressure levels greater than 136 dB measured at approximately 1 inch from the pipe wall would be sufficient to expect fatigue failures.

CASE HISTORIES

Over the past several years, the authors have had the opportunity to evaluate a number of situations where high-frequency vibration was causing high noise amplitudes and fatigue failures. Such problems are seemingly becoming more prevalent, as flow rates through equipment and piping rise. The problems occurred with screw compressors, centrifugal compressors, and roots-type blowers. Excitation mechanisms included blade-passing frequency, pocket-passing frequency, and vortex shedding.

In some cases, the noise problems were treated with acoustical lagging. Other cases were solved by removing the energy generation mechanisms (in the cases of vortex shedding), removing the amplification mechanisms (in cases of blade-pass excitation), installing specially designed silencers, or a combination of these methods. The following sections will briefly present a few of these cases.

Laboratory Testing—Pipe with Zero Flow

A simple laboratory test was conducted in an effort to gain a greater understanding of the phenomena involved in generation and propagation of high-order acoustical modes. The test plan included investigations of high-order mode generation and methods to "turn off" the modes once they were generated.

Excitation of Cross-Wall Modes

A 12 inch diameter (11.875 inch ID), 20 ft long plastic pipe was constructed in the laboratory. A white noise or a swept-sine signal was applied to a speaker that was mounted radially at the pipe wall. Several locations were selected for placement of microphones to measure responses in the pipe (Figure 14). Anechoic terminations were provided at each end of the pipe using acoustical foam inserts.

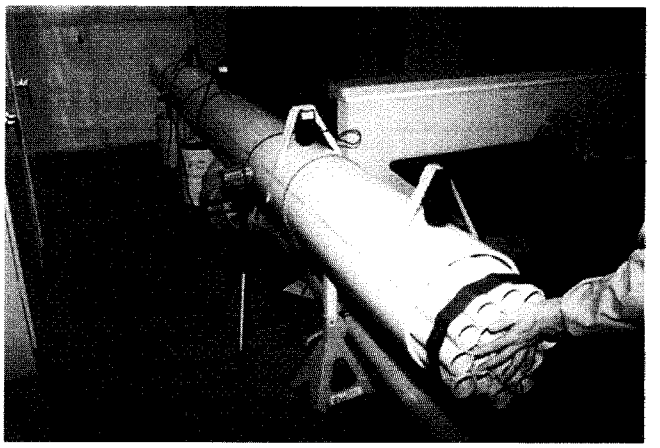

Figure 14. Laboratory Test—Pipe with Zero Flow (Showing Insertion of Tube Bundle).

Cross-wall mode frequencies were calculated for this pipe for m = 1 to 6 and n = 0 to 1. Responses were measured from white noise excitation applied radially at the pipe wall. Agreement between calculated and measured values was good, as shown in Table 2. Note, however, that for this excitation arrangement, only the purely diametrical modes (m = 0 to 6, n = 0) were excited much stronger than the circumferential modes.

Table 2. Predicted/Measured Cross-Wall Modes for Air in 12 Inch Pipe—Radial Excitation.

m	Frequency (Hz)			
	n = 0		n = 1	
	Calc	**Meas**	Calc	**Meas**
0	0		1387	**1388**
1	666	**668**	1929	**1956**
2	1105	**1108**	2427	**2428**
3	1520	**1524**	2900	**2904**
4	1924	**1928**	3359	—
5	2322	**2320**	3807	—
6	2714	**2716**	4246	—

The test was repeated with excitation applied at the pipe centerline (axially). In this configuration, it was much more difficult to excite cross-wall modes. The response data were not as clear (more broadband). However, as shown in Table 3, responses at 1400 Hz, 1950 Hz, and 2450 Hz were measured that corresponded to circumferential modes for the (0, 1), (1, 1), and (2, 1) modes, respectively.

These tests indicated that the diametrical modes seem to be easier to excite than the circumferential modes. Furthermore, the excitation must couple well with the mode shape to "turn on" cross-wall modes.

Elimination of Cross-Wall Modes

Experiments were conducted to determine if the cross-wall mode propagation in the piping could be reduced or eliminated. Several different devices including a perforated disk, an "X-divider," and a bundle of 2 inch tubes (Figure 7) were evaluated. The devices were inserted into the pipe, downstream of the second

Table 3. Predicted/Measured Cross-Wall Modes for Air in 12 Inch Pipe—Axial Excitation.

m	Frequency (Hz)			
	n = 0		n = 1	
	Calc	**Meas**	Calc	**Meas**
0	0		1387	**1388**
1	666	—	1929	**1956**
2	1105	—	2427	**2428**
3	1520	—	2900	—
4	1924	—	3359	—
5	2322	—	3807	—
6	2714	—	4246	—

microphone. Excitation was provided at the pipe wall (radial direction) near the front end of the pipe and the noise data were measured at several locations in the piping.

Response data with the perforated plate showed that this element provided no attenuation of cross-wall modes.

Although the X-divider turned off the cross-wall modes in the section with the X-divider, the modes tended to re-form after leaving the X-divider section. This test indicated that adding X-dividers to the piping could eliminate the cross-wall modes; however, the plates would have to be installed over the full length of the piping, which would probably not be practical.

The tube bundles that were evaluated were similar to flow straighteners used to improve the accuracy of flow meters. The tube bundles consisted of 18, 2 inch diameter pipes. One bundle was 2 ft long (two pipe diameters) and a second bundle was 4 ft long (four pipe diameters). The tests with the tube bundles indicated that both bundles were effective in preventing the formation of the cross-wall modes in the section of piping with the tube bundles. However, the 4 ft length bundle was more effective in preventing reformation and propagation of cross-wall modes downstream of the bundle. This suggested that the commercially available flow straighteners may not be as effective in preventing the propagation of cross-wall modes, due to the short length of the tubes (typically less than one pipe diameter). Note that cross-wall modes could also occur in the 2 inch diameter tubes, but the frequencies would be much higher, and would not be as likely to cause shell wall vibration of the 12 inch piping.

It should be remembered that due to the design of the test facility, these tests were performed with zero mean flow. If there had been flow, some attenuation would have likely been observed through the perforated plates due to the inherent pressure drop. Additionally, the greater attenuation due to pressure drop may have prohibited reformation of cross-wall modes downstream of the X-divider.

Limited information was obtained from these tests. Therefore, it is recommended that additional research should be conducted with more rigorous testing to evaluate the potential for "turning on" cross-wall modes, and to evaluate modifications that could reduce cross-wall mode formation.

Compressor Station—Suction Side

A series of new pipeline compressor stations was experiencing high amplitude, high-frequency noise and vibration of the suction piping associated with the compressors. Failures of instruments on the suction piping near the compressors resulted. Additionally, the noise levels in the buildings were excessive for personnel (> 125 dB), requiring both ear plugs and muffs to be worn.

Each compressor station utilized a centrifugal compressor driven by a gas turbine. The compressors had a single, overhung impeller. Because of flow requirements, some stations utilized a 17-blade impeller while others used a 14-blade impeller. The compressor operating speed range was 3120 rpm to 5040 rpm with a rated speed of 4800 rpm. Design operating pressures were 1050 psi suction and 1460 psi discharge. Suction and discharge piping for the compressors were 36 inch diameter (0.75 wt).

It was hypothesized that the noise and vibration were the result of amplification of energy by high-order acoustical modes in the piping and/or piping shell wall modes. The excitation source was not known; however, blade-pass energy or vortex shedding were considered to be probable mechanisms.

Calculations

The calculations discussed in previous sections, *Acoustic Cross-Wall Natural Frequencies*, and *Shell Wall Natural Frequencies*, were performed to see if there were potential coincidences of acoustical natural frequencies and shell wall natural frequencies with excitation mechanisms.

- *Acoustical cross-wall mode natural frequencies*—Using the equations in the section *Acoustic Cross-Wall Natural Frequencies*, the high-order acoustical modes for the 36 inch (34.5 inch ID) pipe for m = 1 to 32 and n = 0 to 7 were calculated. The results for several of the modes are shown in the table in the section, *Analysis of Measured and Calculated Data.*

- *Piping shell wall mode natural frequencies*—Using the equations in the section, *Shell Wall Natural Frequencies*, the shell wall modes of the piping were calculated and are shown in Table 4. Also shown are the radiation efficiency parameters, calculated using the equations in the section, *Radiation Efficiency*.

Table 4. Shell Wall Modes and Radiation Efficiency.

# Diams	Shell Wall Freq (Hz)	**Pipe → Air**		**Gas → Pipe**	
		Coincidence Freq (Hz)	Freq Ratio	Coincidence Freq (Hz)	Freq Ratio
2	63	242	0.26	263	0.24
3	179	363	0.49	935	0.45
4	342	484	0.71	526	0.65
5	554	605	0.92	658	0.84
6	812	726	1.12	789	1.03
7	1118	847	1.32	921	1.21
8	1470	968	1.52	1053	1.40
9	1870	1089	1.72	1184	1.58
10	2317	1210	1.92	1316	1.76
11	2811	1331	2.11	1447	1.94
12	3352	1451	2.31	1579	2.12
13	3940	1572	2.51	1710	2.30
14	4575	1693	2.70	1842	2.48
15	5257	1814	2.90	1974	2.66
16	5986	1935	3.09	2105	2.84
17	6763	2056	3.29	2237	3.02
18	7586	2177	3.48	2368	3.20
19	8456	2298	3.68	2500	3.38
20	9374	2419	3.87	2631	3.56

It is interesting to note that for this piping geometry, most of the potential shell wall modes will radiate sound efficiently. Furthermore, some of the shell wall modes have nodal patterns that are similar to the predicted acoustical mode at that frequency. For example, the seven-diameter shell wall mode was calculated to be at 1118 Hz. The seven-diameter acoustical natural frequency was predicted to be 1173 Hz (refer to Table 7). These calculations indicate that the acoustical and structural modes of the piping could act together to produce even larger amplifications of energy.

• *Vortex shedding*—Flow velocities calculated from measured plant operational conditions indicated that obstructions of 0.1 inch to 0.5 inch in diameter could produce vortex shedding excitation in the range of the expected acoustical natural frequencies. Obstructions in this size range were thought to exist at the strainer (stiffener rings), and at various flange gaps and stub connections in the vicinity of the strainer (Figure 15).

• *Conclusions from preliminary calculations*—The calculations showed that for the piping geometry and flows, either blade-pass energy or vortex shedding energy could excite acoustical natural frequencies and shell wall natural frequencies of the piping. These calculations therefore tended to verify the hypotheses for the high amplitude noise and vibration.

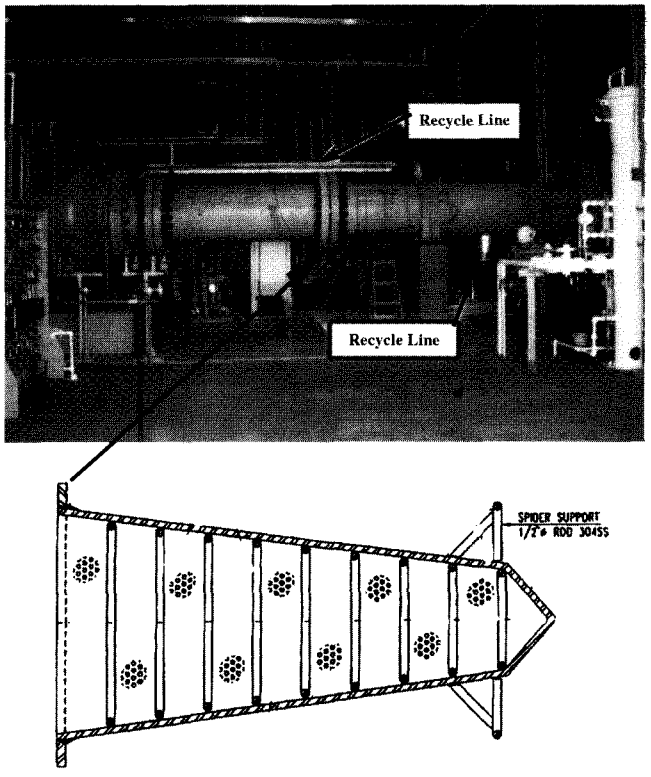

Figure 15. Original Strainer Installation Upstream of Pipeline Compressor.

Field Data—Station 7

Small, high-frequency accelerometers were used to acquire shell wall vibration data. Each accelerometer was attached to a pad, which was glued to the pipe using an adhesive.

Noise data were measured using a sound-level meter (SLM). For the frequency range of interest, these devices are preferred over microphones because of their durability and ease of use. The SLMs were mounted on a tripod and aimed at the pipe. Prior to use, each SLM was calibrated using a 94 dB, 1000 Hz sound source.

Pulsation data were acquired using piezoelectric transducers, installed in insertion probes (refer to section *Insertion Probes*).

Shaft vibration data were recorded from the permanently installed proximity probes. These instruments record radial or axial shaft vibration. A once-per-revolution (key-phase) pulse was also used to monitor compressor speed.

The installed station transducers and process computer provided additional data (suction pressure, discharge pressure, temperatures, gas composition, etc.).

• *Operating data*—The compressor was operated over the operating speed range achievable on the day of the test. All data were tape recorded during the test for later analysis.

A trending program was set up to monitor process data during the tests. The compressor speed, station flow, and suction and discharge pressures during the test are shown in Figure 16. As shown, the speed ramp of 3120 rpm to 4400 rpm took place during an interval of approximately 20 minutes. Suction pressures ranged from 1140 psi to 1045 psi, while discharge pressures went from 1298 psi to 1392 psi. Station flow was varied from 1760 MMscfd to 2500 MMscfd.

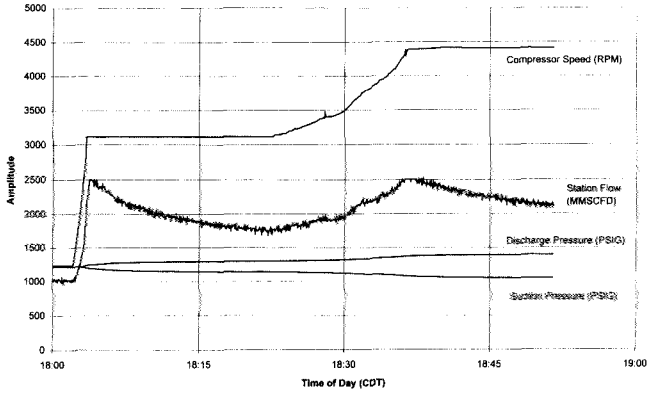

Figure 16. Station 7 Operating Conditions During Testing.

Using station flow, temperature, gas properties, and pressure data, the average flow velocities in the suction pipe during the test were computed. As shown in Figure 17, the average flow velocity in the suction pipe ranged from approximately 32 ft/sec to nearly 50 ft/sec. For the period of the testing, the flow velocity varied essentially linearly with compressor speed.

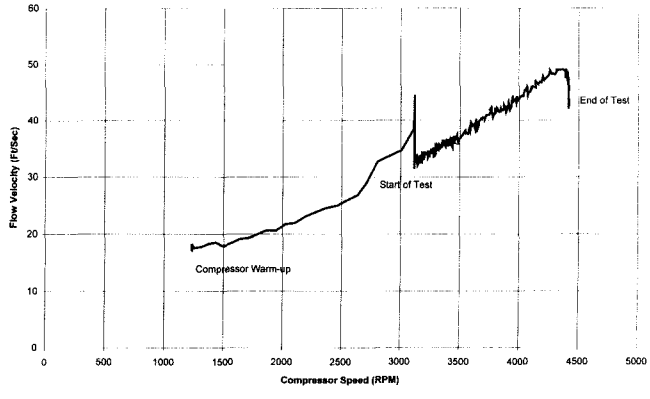

Figure 17. Average Flow Velocity Versus Compressor Operating Speed.

Waterfall plots were made for the recorded data. As shown in Figure 18, the suction line pulsation data measured downstream of the strainer show discrete frequency peaks that line up vertically. These peaks were especially apparent in the data acquired downstream of the strainer.

Excitation at blade-pass frequency (17× running speed) and 2× blade-pass frequency (34× running speed) can be seen as peaks

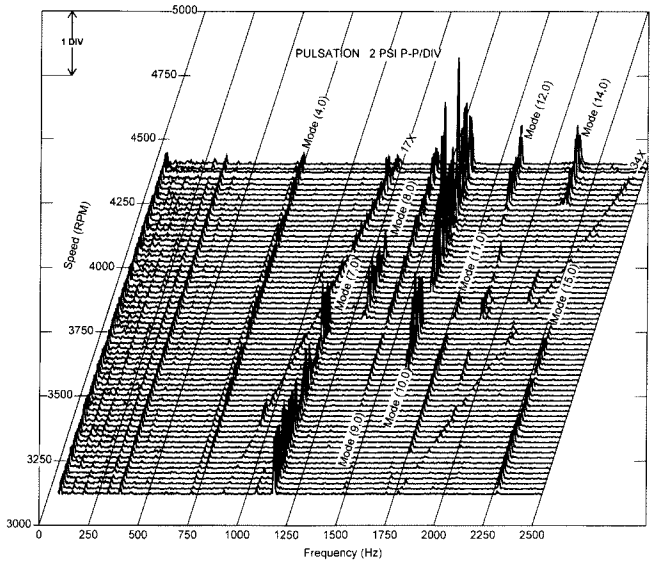

Figure 18. Suction Line Pulsation Measured Downstream of Strainer—Station 7.

that lie along the 17× and 34× order lines. However, these peaks were typically much lower amplitude than the vertically aligned ones. This behavior suggests the presence of acoustical resonances (cross-wall modes) at the frequencies of the vertically aligned peaks.

Another behavior that can be observed from the data is that as compressor speed (and as shown by Figure 17, flow velocity) increases, peaks at lower frequencies die out while new peaks at higher frequencies appear. These data show that acoustical resonances (vertically aligned peaks) were being excited by vortex shedding, since the vortex shedding phenomenon generates banded energy at higher frequencies for higher flow velocities.

Discharge pulsation data (Figure 19) show behavior similar to the suction side, but at much lower amplitudes. Broadband turbulent energy and blade-pass excitation predominate these data.

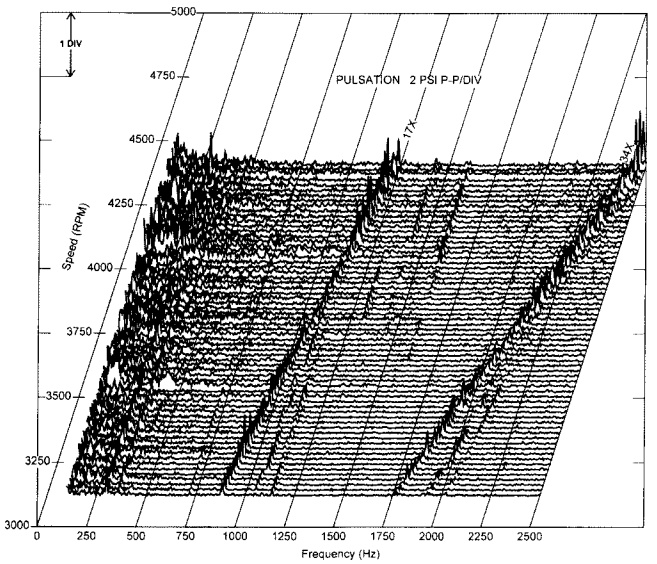

Figure 19. Discharge Line Pulsation Measured near Compressor—Station 7.

The noise data and the measured shell wall vibration of the suction and discharge piping indicated that most of the vibration and noise were caused by pulsation in the suction pipe. Vibration amplitudes were measured to be as high as 100 g's zero-peak at several different frequencies. While these levels were not thought to be sufficient to cause failures of the piping itself, attachments to the piping (thermowells, pressure connections, instruments, etc.) could be expected to fail.

Shaft vibration data showed that the vibrations were low amplitude. Furthermore, the majority of the vibration was at the first few multiples of running speed. However, a few low amplitude peaks were apparent in the axial vibration data that corresponded to pulsation in the suction piping. These data showed that the pulsation and piping vibration were not adversely affecting shaft vibration.

- *Impact data*—With the compressor shut down, impact response data of the suction and discharge piping were gathered. Both the impact and response were in a radial direction.

The impact tests produced a large number of response peaks (Figure 20). However, the peaks were in distinct groups. Although a full modal analysis was not done, experience has shown that the individual peaks in these groups of natural frequencies will probably have similar mode-shapes (e.g., a five-diameter mode), but are at slightly different frequencies due to local discontinuities such as branch connections or weldolets.

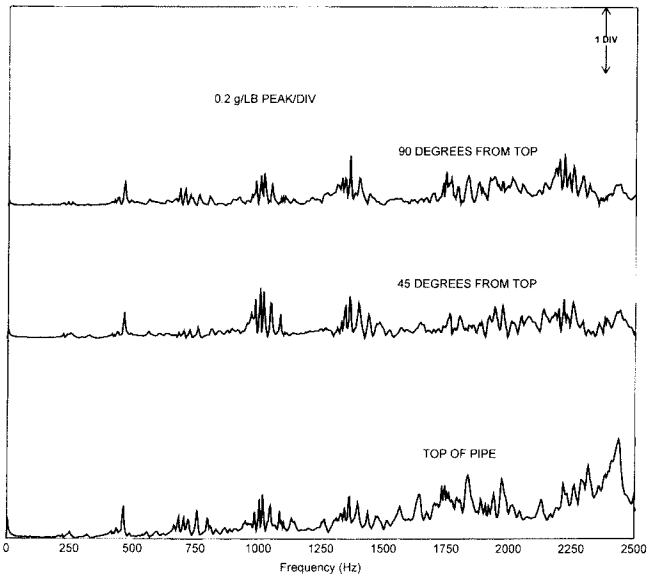

Figure 20. Impact Response Data of Suction Piping Shell Wall Near Strainer.

The measured shell wall natural frequencies (from impact tests) did not correlate well with the measured shell wall vibration peaks (when operating), although some frequencies were in close proximity. These data indicate that the piping shell wall vibration was not being significantly amplified by structural natural frequencies.

Field Tests—Station 9

Similar testing was performed at Station 9. This station had higher flow rates than the Station 7. The compressor had an impeller with 14 vanes.

As shown in Figure 21, pulsation data showed that Station 9 was also experiencing high pulsation due to excitation of cross-wall acoustical modes. For purposes of this paper, the remainder of the data is not presented in detail, but will be included in summary for comparison purposes.

Analysis of Measured and Calculated Data

As shown in Table 5, there was good agreement between the measured pulsation frequencies and the calculated cross-wall acoustical natural frequencies. These data confirm that the measured pulsation was the result of excitation of cross-wall acoustical modes in the piping.

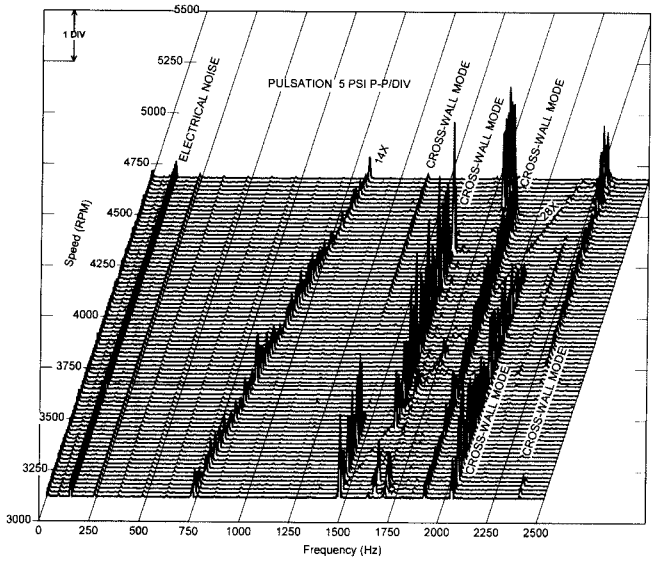

Figure 21. Suction Line Pulsation Measured Downstream of Strainer—Station 9.

Table 5. Comparison of Measured and Calculated Cross-Wall Modes.

Mode No. (m, n)	Calculated Values	Measured Frequencies	
		Station 7	Station 9
	Frequency (Hz)	Frequency (Hz)	Frequency (Hz)
(4, 0)	727	—	—
(5, 0)	877	—	—
(6, 0)	1026	—	—
(7, 0)	1173	1126	—
(8, 0)	1319	1297	—
(9, 0)	1465	1431	1460
(10, 0)	1609	1607	1630
(11, 0)	1754	1752	—
(12, 0)	1898	1853	1890
(13, 0)	2041	—	2027
(14, 0)	2184	2132	2281
(15, 0)	2327	—	2376

In situations where variable frequency energy excites system natural frequencies, "interference diagrams" can be used to help understand the coincidence of excitation and resonance. Lines are plotted on the diagram representing system resonances. Additional lines are plotted that show variable frequency excitation. Points of intersection between excitation lines and system resonances indicate areas where the energy can excite a resonance. Such an interference diagram was generated and is shown in Figure 22.

The vertical axis is assigned to be frequency in Hz. Natural frequencies (n = 0 cross-wall modes) were plotted with horizontal dashed lines intersecting the vertical axis. These lines correspond to the "Calculated Values" column of Table 5.

For this case, the variable frequency energy is provided by vortex shedding, which is a function of the obstruction diameter and geometry (which are constant), and flow velocity (which is variable). Therefore, by assigning the horizontal axis to represent flow velocity, diagonal lines were plotted to represent the variable frequency excitation for a particular obstruction size.

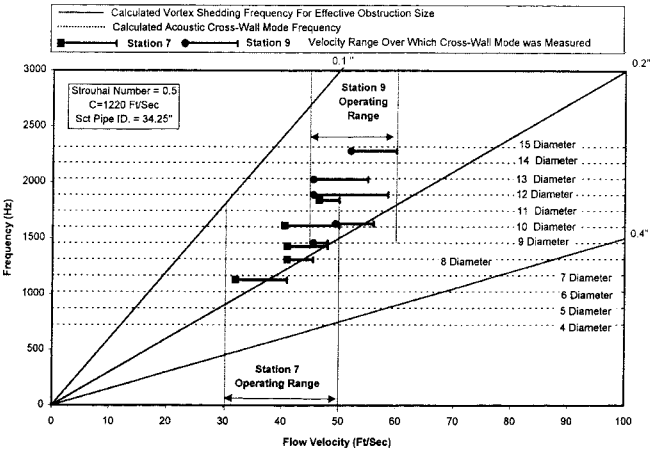

Figure 22. Interference Diagram for Stations 7 and 9—Cross-Wall Acoustic Natural Frequencies and Vortex Shedding Frequencies.

For this diagram, the variable frequency lines are calculated vortex shedding frequencies for a Strouhal number of 0.5 and flow velocity of zero to 100 ft/sec. Three diagonal lines are shown representing a potential for energy generation for obstruction sizes of 0.1 inch, 0.2 inch, and 0.4 inch.

For example, a 0.2 inch obstruction in a 100 ft/sec flow stream will generate energy near 3000 Hz. The same obstruction in a 30 ft/sec flow stream will generate energy near 800 Hz. The diagonal line drawn through these points shows excitation over a range of flow velocities.

Measured pulsation responses were plotted along this diagram to estimate obstruction size. The measured cross-wall natural frequencies (from the "Measured Frequencies") columns of Table 5 were plotted using horizontal lines with square ends. The length of these lines show the velocity where the particular cross-wall mode turned on or off. Dotted vertical lines are shown to represent the range of velocities over which the compressor operated.

With all these data plotted, an imaginary excitation line was drawn through the middle of the measured cross-wall mode ranges. This line represents an estimated obstruction size. Therefore, using this interference diagram, an obstruction size of 0.15 inch to 0.2 inch was predicted. Note however that this was based upon average flow velocities around a cylinder, oriented perpendicular to the flow. Since all these factors are approximations, the actual obstruction size may have been somewhat different. However, these data provided an indication of the range of obstruction sizes that could have been causing the vortex shedding.

Conclusions

Based upon the measured data and calculations, it was concluded that the strainer was generating vortex shedding energy that was being amplified by cross-wall acoustical modes in the piping. Stiffener rings on the strainer had approximately the correct dimensions to produce the vortex energy. However, it was not completely proven that these rings generated the vortex energy.

It was recommended that a modification be considered that would both reduce the potential for vortex energy generation, and also prevent acoustical cross-wall formation in the frequency range of interest.

Modification

The proposed strainer modification is shown in Figure 23. The stiffener rings were removed and longitudinal plates were added to prevent the formation of acoustical cross-wall modes, and provide structural support for the perforated metal of the strainer. The perforated metal was rolled at the edges to reduce stress concentration at the attachment point to the longitudinal plates.

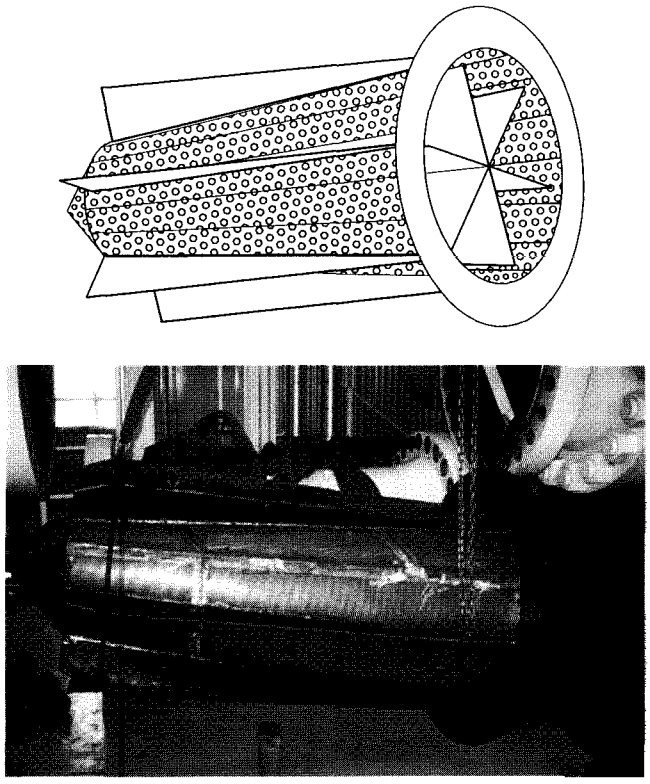

Figure 23. Proposed Strainer Modification.

This modified strainer was installed at Station 9. Upon startup, it was immediately obvious that the strainer modification had solved the noise problem.

Pulsation, noise, and vibration data were acquired with the compressor operating and the modified strainer installed. As shown in Figure 24, the high-frequency vertically aligned peaks in pulsation were still present, but they were greatly reduced in amplitude (compare Figure 21 with Figure 24). Note that the blade-pass energy pulsation (14× running speed) was approximately the same before and after modification.

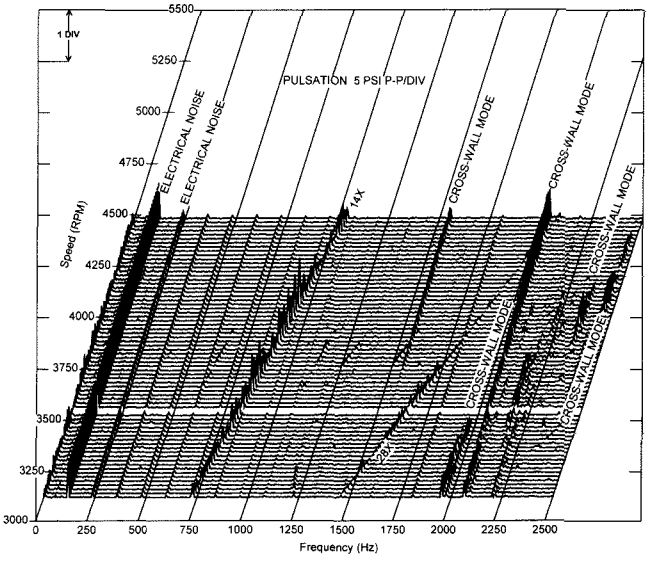

Figure 24. Suction Line Pulsation after Installation of Modified Strainer—Station 9.

The suction pulsation levels were reduced by a factor of six (12 psi peak-to-peak to 2 psi peak-to-peak). Piping vibration amplitudes downstream of the silencer were reduced by a factor of 25 (125 g's zero-peak to 5 g's zero-peak). Noise levels were also reduced to acceptable levels.

Based upon these data, it was concluded that the strainer modification prevented formation of the cross-wall modes in the piping section where the strainer was installed. These modes apparently re-formed either upstream or downstream of the strainer, indicating that some vortex shedding was still occurring in the system. However, the vibration and noise levels were much lower with the modifications.

This case history illustrates potential problems with strainers and other obstructions installed in the piping. In situations such as these where an obstruction is intended to be permanently installed, the possibility for vibration and noise problems should be considered. Calculations of coincidences between potential vortex shedding frequencies, shell wall modes, and acoustical cross-wall modes should be performed in the design stage. Note, however that additional factors not included in such calculations (such as flow angles, location of the obstruction, damping, attached small-bore piping, etc.) can, in practice, significantly influence whether such coincidences will actually combine to cause noise and vibration problems.

Compressor Station—Discharge Side

A pipeline compressor station was experiencing excessive vibration and noise levels on the discharge piping. Even though the compressor was installed in an enclosed, acoustically insulated building, nearby residents were complaining of excessive noise. The noise levels measured near the house were approximately 70 dBA. The Federal Energy Regulatory Commission (FERC) noise requirements are 55 dBA LDN, which for a continuous source is equivalent to 48 dBA.

The single-stage overhung centrifugal compressor was driven by an electric motor through a speed increaser. The motor was equipped with a variable frequency drive (VFD) that allowed the compressor speed to be varied over a speed range of approximately 4600 rpm to 6700 rpm.

Field tests indicated that the noise levels were predominantly at the compressor vane-passing frequency (17× running speed) and twice the vane-passing frequency (34× running speed). The maximum noise levels occurred at approximately 1900 Hz (17×) when the compressor was running near 6600 rpm. The overall sound levels in the building were approximately 114 dBC.

Measured data and calculations revealed that the excessive noise levels were due to the coincidence of acoustical cross-wall natural frequencies and mechanical shell wall natural frequencies of the piping. Pulsation at the compressor blade-passing frequencies was amplified by the cross-wall natural frequencies. The piping vibration due to the pulsation at the blade-passing frequencies was further amplified by the shell wall natural frequencies of the piping, resulting in high amplitude shell wall vibration and excessive noise levels.

Cross-Wall Natural Frequencies

The discharge pulsation amplitudes generated by the compressor were approximately 0.2 psi to 0.5 psi peak at the blade-passing frequency (17×), and 0.1 psi to 0.2 psi peak-to-peak at twice the blade-passing frequency (34×). These pulsation amplitudes were considered to be typical for compressors of this type. The pulsations generated by the compressor at the blade-passing frequencies were amplified when the vane passing frequencies were coincident with the cross-wall natural frequencies of the piping.

A comparison of the calculated acoustic cross-wall natural frequencies with the measured pulsation response frequencies is shown in Table 6. As shown, the calculated diametrical modes favorably agreed with the acoustic natural frequencies excited by the pulsation at multiples of the compressor blade-passing frequency. Acoustic natural frequencies up to the sixteenth mode near 3700 Hz were measured.

Table 6. Comparison of Calculated and Measured Cross-Wall Natural Frequencies in 26 Inch Piping (wt = 0.5 in).

Calculated		Measured Pulsation	
Mode (m, n)	Frequency (Hz)	Frequency (Hz)	Pulsation psi, p-p
Excited by Energy at 17×			
(2, 0)	625	650	1.5
(3, 0)	860	950	1.5
(4, 0)	1089	1125	1.5
(5, 0)	1313	1325	6.0
(6, 0)	1536	1550	1.0
(7, 0)	1775	1800	1.5
(8, 0)	1975	1900	2.0
Excited by Energy at 34×			
(9, 0)	2202	—	—
(10, 0)	2422	—	—
(11, 0)	2642	2600	0.5
(12, 0)	2861	2850	1.0
(13, 0)	3081	—	—
(14, 0)	3301	—	—
(15, 0)	3521	3600	0.5
(16, 0)	3698	3750	1.0

Quarter Wave Stub Natural Frequencies

The pulsation data summarized in Table 6 were obtained with an insertion probe. As shown, the pulsation amplitudes were in the range of 0.5 psi peak-to-peak to 6 psi peak-to-peak. However, pulsation data obtained by installing pressure transducers at the end of stubs indicated pulsation levels of approximately 100 psi peak-to-peak at the quarter wave stub natural frequencies. These pulsation data illustrate the importance of using insertion probes when acquiring high-frequency pulsation data.

An example of pulsation due to the quarter wave stub resonances is shown in Figure 25. The pulsations were measured at a thermowell test location in the flange that resulted in a stub with an effective length of approximately 9.4 inch between the pressure transducer and the inside of the pipe. The stub resonances were excited by pulsation at 17× running speed. As shown, the stub created major acoustic responses with pulsation levels of approximately 25 psi peak-to-peak at 600 Hz, 125 psi peak-to-peak at 1400 Hz, and 75 psi peak-to-peak at 1800 Hz.

These quarter wave stub responses were verified by computing the acoustic natural frequencies of the stub. The computer model included the tubing fittings, the stub (thermowell), and a short section of the discharge piping (Figure 26). The computed response frequencies and pulsation amplitudes favorably agreed with the measured pulsation data, which also verified that the high amplitude responses measured at the end of the stubs were acoustic natural frequencies of the stubs, and were not cross-wall natural frequencies of the discharge piping. The pulsation amplitudes at the stub resonances were maximum at the closed end of the stub at the pressure transducer and were almost zero at the open end of the stub at the main piping (Figure 27).

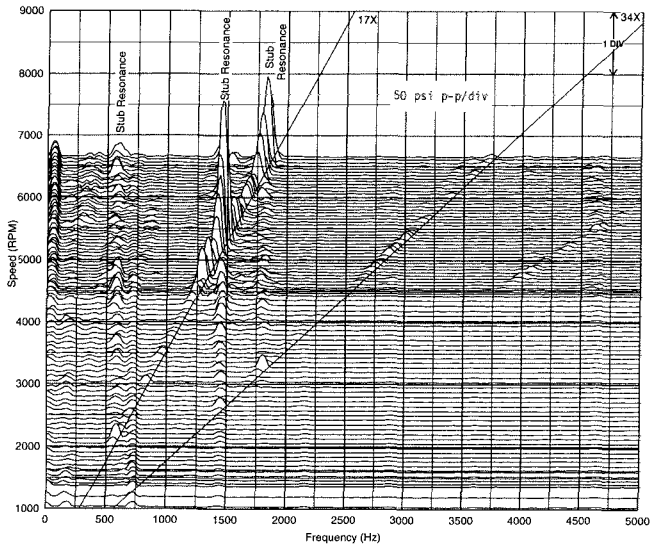

Figure 25. Pulsation Due to Quarter-Wave Stub Resonances.

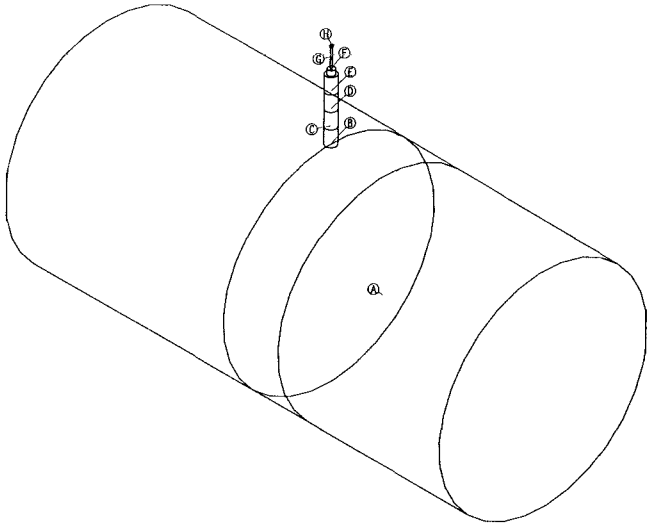

Figure 26. Computer Model of Thermowell Pressure Tap.

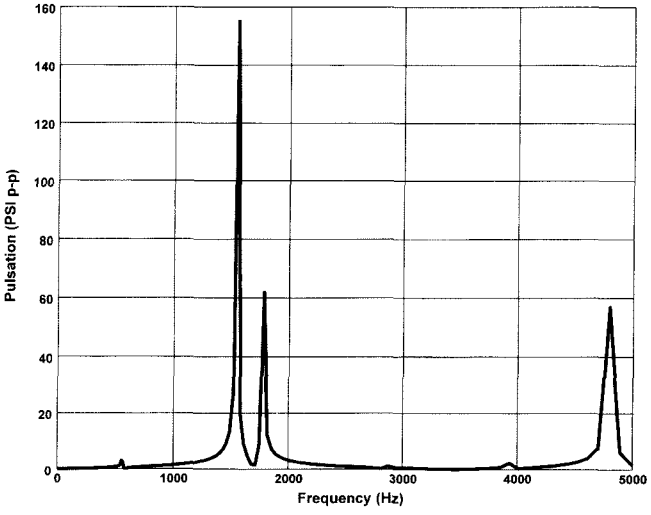

Figure 27. Computed Passive Acoustic Frequency Response for Thermowell.

Although pulsations at the stub frequencies are considered to be measurement errors when measuring pulsation in the main piping, the high pulsation in the stubs is also a potential source of high-frequency energy that can excite the piping shell wall mechanical natural frequencies. The available shaking force can be estimated by multiplying the cross-sectional flow area (in^2) by the pulsation amplitude (lb/in^2) (Force = area H pulsation). For example, the shaking forces at the closed end of a 1 inch diameter thermowell with 100 psi peak-to-peak pulsation would be approximately 80 lb peak-to-peak. This is a significant high-frequency shaking force, which can excite the shell wall natural frequencies. Therefore, the number and lengths of stub connections should be minimized.

Shell Wall Natural Frequencies

Impact tests were performed to measure the shell wall mechanical natural frequencies of the suction piping, discharge piping, and suction scrubber. The piping was impacted with a steel tipped instrumented hammer to excite the high-frequency shell wall natural frequencies. The responses at the shell wall natural frequencies were measured with accelerometers, strain gauges, and sound level meters. The accelerometers were mounted on pads that were glued to the piping. The strain gauges were installed near the accelerometers and were oriented to measure the strain in the circumferential direction (hoop stress). The sound level meters were mounted on tripods near the piping. The shell wall responses measured with the accelerometers, strain gauges, and sound level meters favorably agreed (Figure 28).

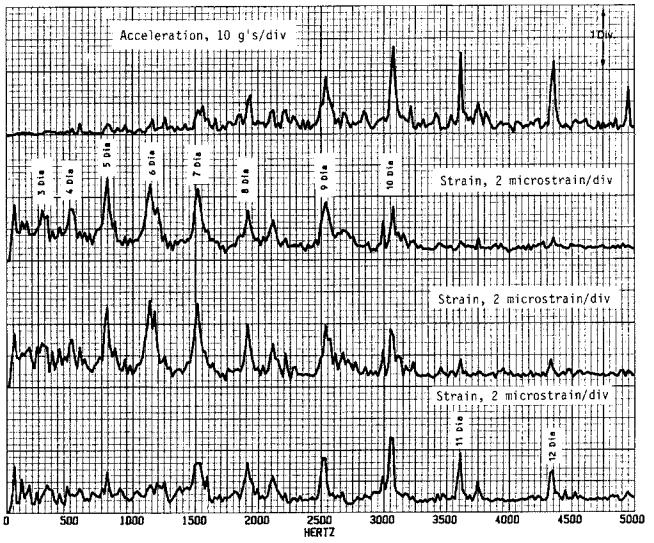

Figure 28. Measured Shell Wall Natural Frequencies Due to Impacts.

The frequencies of several of the discharge piping shell wall natural frequencies increased when the piping was pressurized to 825 psi. The increase in natural frequencies was due to stiffening effects from the internal pressure. The computed and measured shell wall natural frequencies for the 26 inch diameter discharge piping are compared in Table 7. As shown, the increase in natural frequencies due to the pressure could be approximated by increasing the wall thickness (wt) by 10 percent to 0.55 inch. The good agreement between the measured and calculated frequencies confirmed that equations in the section, *Shell Wall Natural Frequencies*, can be used to approximate the shell wall natural frequencies.

The maximum piping vibration levels measured on the discharge piping were approximately 100 g's peak-to-peak near 1900 Hz

Table 7. Comparison of Calculated and Measured Shell Wall Natural Frequencies in 26 Inch Piping (wt = 0.5 in).

Number of Diameters	Computed		Measured	
	wt = 0.5 in	wt = 0.55 in	P = 0 psi	P = 825 psi
2	80	89	—	—
3	227	251	250	270
4	436	482	450	500
5	705	779	740	800
6	1035	1142	1070	1150
7	1424	1572	1470	1500
8	1873	2069	1950	1950
9	2383	2631	2450	2540
10	2952	3260	3000	3050
11	3581	3955	3600	3600
12	4270	4716	4250	4350

(17× at 6700 rpm) (Figure 29). These piping vibration levels were not considered to be excessive with regard to fatigue failures of the main piping; however, the resulting noise levels were excessive. Furthermore, experience has been that such vibration levels can cause failures of small diameter lines and instrumentation attached to the piping.

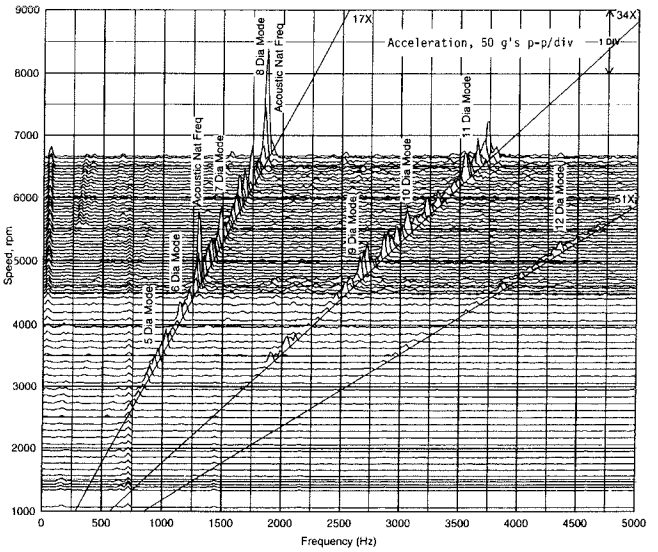

Figure 29. Discharge Piping Shell Wall Vibration During Startup.

Although the pulsation levels were higher at the cross-wall natural frequency near 1300 Hz, the maximum vibration, strain, and noise levels occurred at the resonance near 1900 Hz. The test data and the calculations indicated that the eight-diameter shell wall mechanical natural frequency and the eighth diametrical (8, 0) cross-wall acoustic natural frequency were both coincident with the vane passing frequency when the compressor was operating at approximately 6700 rpm. This suggests that the shell vibration levels were easier to excite when the pulsation mode shape matched the mechanical mode shape.

Pipe Clamp Mechanical Natural Frequencies

The maximum noise levels were measured near a large thermal stop pipe clamp at the compressor discharge nozzle (Figure 30). The vibration levels were approximately three times higher on the pipe clamp compared with the levels on the pipe wall. Impact tests on the pipe clamp revealed several mechanical natural frequencies near 1900 Hz. The shell wall vibration of the discharge piping at 1900 Hz excited the mechanical natural frequencies of the pipe clamp. The vibration of the pipe clamp caused the noise levels to be further increased. As shown in the photograph, this thermal stop pipe clamp was not originally treated with sound insulation.

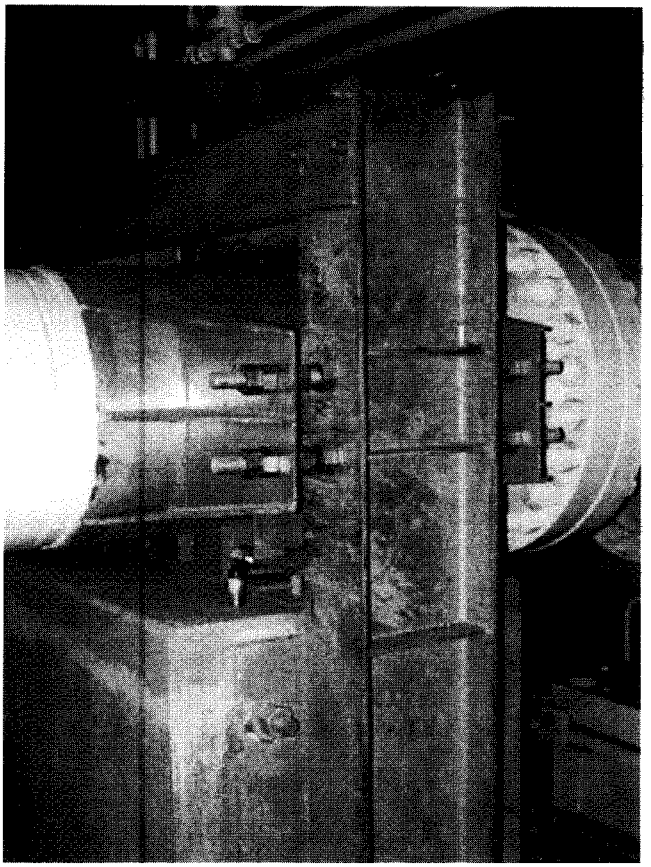

Figure 30. Pipe Clamp on Discharge Piping. (Note: The clamp was later treated with sound insulation.)

Noise Treatment

The preferred modification to reduce the excessive noise levels was to reduce the discharge pulsation energy at the blade-passing frequencies, which was the source of the piping vibration and noise. One possibility was to install a high-frequency pulsation filter in the discharge piping; however, it would require major piping modifications to install the filter. Another possibility was to prevent the amplification of the pulsation by eliminating the cross-wall natural frequencies at the blade-passing frequencies by installing modifications inside the discharge piping, such as the tube bundle discussed in the section, *Prevention of Cross-Wall Acoustical Modes*. However, due to time limitations, the tube bundles could not be installed.

Since the measured strain levels were considered to be low with regard to potential fatigue failures of the main piping, it was decided that noise treatment would be installed to reduce the noise levels, rather than reducing the pulsation and vibration levels. Additional noise treatments were installed on all the inside discharge piping, the pipe clamps, the scrubber, and the outside block valves and control valves. The following modifications were installed.

- On the outside yard piping, an extra layer of sound treatment was installed over the existing sound insulation, which was similar to the noise insulation shown in Figure 10. The final configuration consisted of the following: 4 inch of glass fiber adjacent to the pipe wall, a sound barrier jacketing, a vinyl layer, 2 inch of glass fiber, and another sound barrier jacketing.
- The discharge piping and clamps inside the compressor building were lagged with noise insulation similar to Figure 10.
- Sound blankets were installed on all vents, block valves, control valves, and check valves.
- The suction scrubber and the attached inlet and outlet piping were lagged with noise insulation similar to Figure 10.
- The seal between the building and the discharge piping was removed to prevent the piping vibration levels from being mechanically transferred to the building walls where the noise levels could be radiated from the building walls.
- Seals were installed under the building doors to prevent the noise from passing though the cracks under the doors.

After these modifications were installed, the noise levels at the nearby house were reduced to acceptable levels. No noise treatment was installed on the suction piping inside the compressor building, because the test data indicated that the pulsation and vibration levels were very low in the suction piping. It is felt that the pulsation levels were significantly lower on the suction side of the compressor due to the geometry of the compressor case that prevented the pulsation from being directly transferred into the suction piping.

Refinery—Compressor Wheel Failure

The compressor wheel of an overhung, motor driven centrifugal compressor had experienced cracking at four locations on the wheel. The compressor wheel had 17 blades, and was operated at a constant speed of 4558 rpm (76 Hz).

The location of the failures corresponded with node lines of a three-diameter structural natural frequency of the compressor wheel (Figure 31). Therefore, it was suspected that excitation of a compressor wheel natural frequency might have caused the failures. An experimental modal analysis of the compressor wheel was conducted to determine if one of its natural frequencies coincided with running speed or blade-pass excitation.

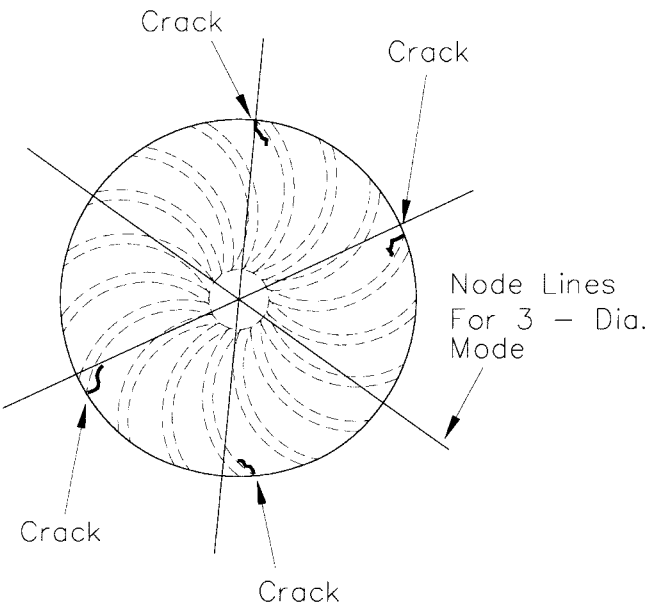

Figure 31. Location of Compressor Wheel Fatigue Failures.

During the impact testing, the compressor wheel was supported by a mandrel and hung from an overhead crane. The number of test point locations was selected to provide information for structural modes having up to four diametrical (m) and two annular (n) node lines. A 1 lb instrumented hammer was used to excite the wheel. Response data were obtained at each test point location from a 0.8 oz wax-mounted accelerometer.

The modal analysis identified several wheel natural frequencies, three of which are shown in Table 8. Since blade-pass excitation was 1292 Hz, it appeared initially that the (3, 0) wheel mode would not be excited, and therefore could not be the cause of the failures. However, pulsation data were acquired to determine if other energy sources were present.

Table 8. Compressor Wheel Mode Natural Frequencies.

Wheel Mode (m, n)	**Natural Frequency** (Hz)
(2, 0)	511
(3, 0)	1140
(4, 0)	1610

Pulsation data acquired at the inlet to the compressor showed a strong response peak at 1140 Hz (Figure 32). Note that the pulsation data were not acquired with an insertion probe. Therefore, several stub frequency peaks can be seen in the data. While the pulsation at 1140 Hz would provide the excitation necessary to excite the (3, 0) compressor wheel mode (and hence cause the failures), it was unknown what was generating the pulsation energy.

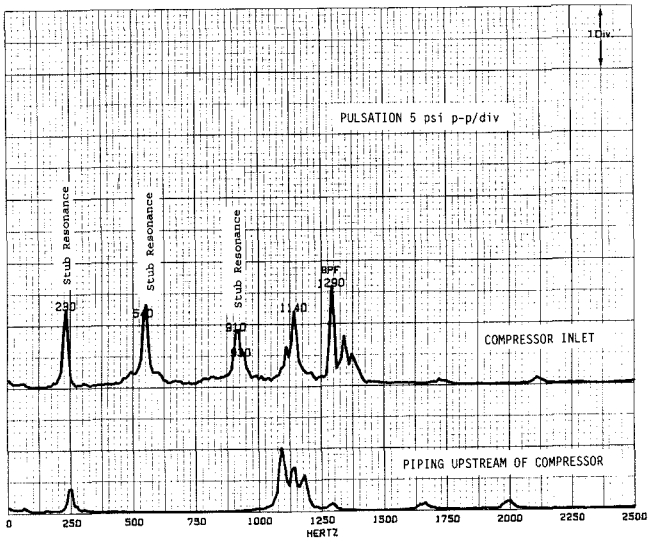

Figure 32. Pulsation Data at Compressor Inlet.

Since a butterfly valve was located just upstream of the compressor inlet, it was hypothesized that vortex shedding from this valve might be exciting high-order acoustical modes in the inlet piping, thereby generating the measured pulsation energy. Using the equations in the section, *Acoustic Cross-Wall Natural Frequencies*, the high-order acoustical modes for this pipe were computed and are presented in Table 9. As shown, the calculations predicted a high-order (1, 2) mode at 1137 Hz.

The measured pulsation data and the results of the calculations seemed to confirm the hypothesis that vortex shedding energy generated by the butterfly valve was exciting a high-order cross-wall

Table 9. Cross-Wall Acoustical Natural Frequencies.

n →	**High-Order Acoustical Natural Frequency** (Hz)			
	0	1	2	3
m = 0	0	510	934	1355
m = 1	245	710	**1137**	1559
m = 2	407	893	1327	1754
m = 3	559	1067	1511	1942
m = 4	708	1236	1689	2126

acoustical mode, which in turn excited the (3, 0) structural mode of the compressor wheel, ultimately causing the experienced failures. It was therefore suggested that the butterfly valve be relocated further upstream of the compressor, or that longitudinal vanes be installed downstream of the valve to "turn off" the high-order cross-wall mode.

Since this valve was not mandatory to the process, plant personnel decided to remove the valve completely during a planned outage. After the valve was removed and the process restarted, pulsation data were acquired. The data showed that the pulsation energy peak at 1140 Hz was no longer present. The unit has been operating without failures for several years since the valve was removed.

LNG Plant—Turning Vane Failure

A refrigeration compressor experienced a catastrophic failure after turning vanes in the first interstage crossover piping failed and were ingested by the second stage impeller. The compressor operates on 100 percent nitrogen in a closed loop process (Figure 33).

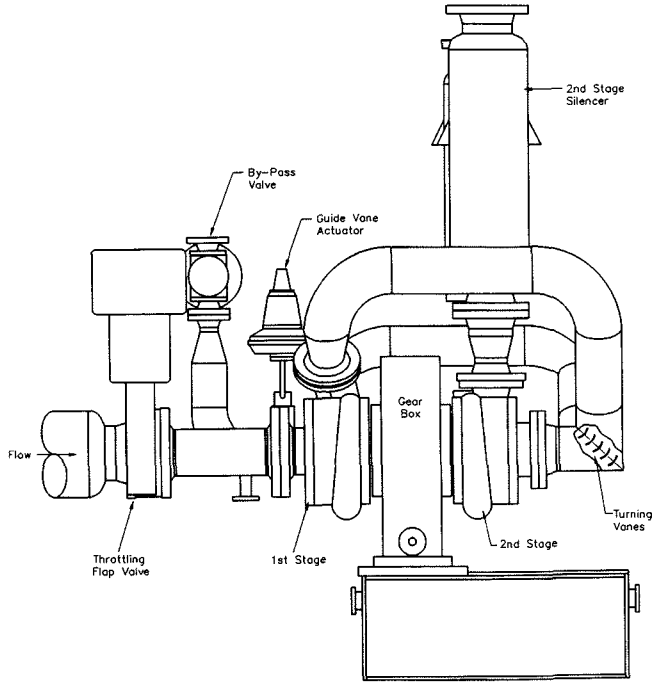

Figure 33. Refrigeration Compressor (First and Second Stages).

The compressor was driven by an induction electric motor at approximately 3000 rpm (50 Hz). The first and second stage impellers are mounted on the low speed pinion shaft, which operates at approximately 20,540 rpm (342.3 Hz). Similarly, the third and fourth stage impellers are mounted on the high-speed pinion shaft that operates at approximately 28,400 rpm (473.3 Hz).

After operating for approximately 250 hours, the compressor experienced a major failure of the second stage impeller and pinion shaft when a piece of one of the second stage turning vanes broke off and entered the second stage impeller. The second stage impeller was damaged, which caused the vibration levels on the second stage pinion to increase suddenly due to the increased unbalance. When the compressor was shut down, the vibration amplitudes increased to excessive levels as the pinion shaft coasted down through its first lateral natural frequency. When the compressor was disassembled, it was determined that major damage had occurred on the second stage impeller, pinion shaft, and seals.

Inspection of the turning vanes revealed that each of the five turning vanes was cracked where the vanes were welded to the pipe. Metallurgical examination of one of the vanes confirmed that the cracks were fatigue cracks that appeared to be initiated at surface pits on the concave surface near the edge of the vane adjacent to a weld. A sketch of the typical vane cracks is shown in Figure 34. The propagation pattern of the cracks suggested that the cracks were probably due to the excitation of a particular mechanical natural frequency, because the location and shapes of all the cracks were very similar. In addition, the cracks did not propagate along the fixed edges of the vanes that would probably be the location of maximum stress for a simple bending of the vane.

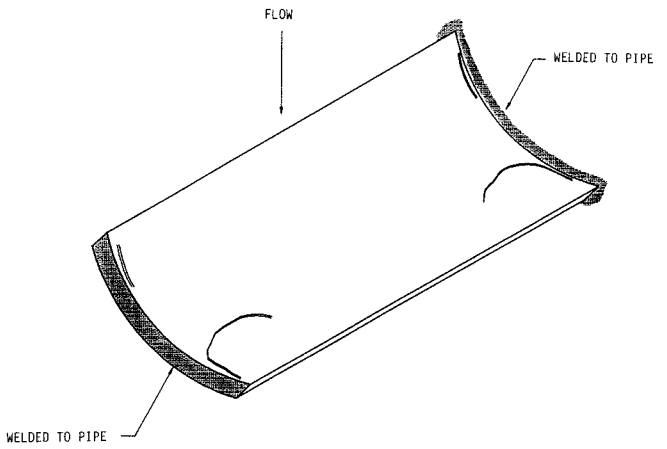

Figure 34. Turning Vane Failure Locations.

Due to the problems with the second stage turning vanes, the fourth stage turning vanes were also examined for cracks; however, no cracks were found in these vanes. This indicated that the failures of the second stage turning vanes could be associated with the reported high vibration levels on the interstage piping between the first and second stages. The vibration levels were reported to be particularly high near the miter joint at the entrance to the second stage impeller (as shown in Figure 33, the turning vanes are inside the miter joint).

Mechanical Natural Frequencies of the Turning Vanes

In an effort to solve the failures of the turning vanes, a new miter joint was fabricated with thicker vanes. The thickness of the new vanes was increased from 4 mm to 6 mm.

Prior to installing the new miter joint, the mechanical natural frequencies and vibration mode shapes of the turning vanes were measured using impact testing. Each of the vanes was divided into a grid with 25 test points. Each vane was impacted near the middle of the vane with an instrumented hammer. A small (1 gram) accelerometer was used to obtain the vibration data at each of the 25 test points. The accelerometer was attached using wax.

Each of the turning vanes had several mechanical natural frequencies between 1000 Hz and 10,000 Hz. The impact tests were made prior to running the compressor; therefore, it was unknown which of the many mechanical natural frequencies could be excited. Initially, it was felt that the turning vane failures could possibly be due to excitation of one or more of the mechanical natural frequencies by pulsation at the impeller vane-passing frequency at approximately 5477 Hz (20,540 rpm × 16 vanes = 328,640 cpm = 5477 Hz). Therefore, the modes near the vane-passing frequency were analyzed in greater detail. However, data obtained during operation indicated that the pulsation and strain levels at the vane-passing frequency were low, which indicated that the failures were not due to excitation at the vane-passing frequency.

Strain and Pulsation Data During Operation

Strain gauges were installed on each of the vanes before the new miter joint was installed (Figure 35). Since the strain gauges were installed inside the piping, the wires to the strain gauges had to be routed through special fittings to provide a pressure seal.

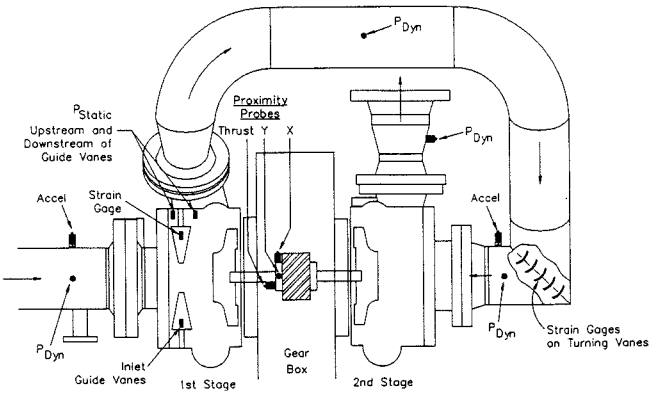

Figure 35. Instrumentation Test Locations.

Pulsations were measured at several locations in the piping using dynamic pressure transducers that were installed using short pipe fittings to minimize the quarter wave stub effects (Figure 35).

The flow rates through the compressor were controlled using variable inlet guide vanes (IGVs), which were installed upstream of the first stage impeller. The bypass valve discharged into the first stage inlet piping just upstream of the IGVs. The IGVs were designed to throttle the inlet flow and to direct the flow into the first stage impeller.

Strain and pulsation spectra were plotted versus time as the inlet flow was varied. When the bypass valve was fully opened, the strain levels on the top turning vane increased to approximately 400 microstrain peak-to-peak (Figure 36). These strain levels were considered to be excessive and could result in fatigue failures. The strain levels were primarily at a response near 2100 Hz, which was one of the vane mechanical natural frequencies. This mechanical natural frequency was excited by the pure tone pulsation near 2100 Hz (Figure 37).

The turning vane mechanical natural frequencies appeared to be excited by flow induced pulsation that was coincident with the vane mechanical natural frequencies. It was thought that the pulsations were due to low amplitude energy vortices formed by flow across an obstruction (vortex shedding).

As shown in Figure 37, the pulsation frequencies shifted as the bypass valve position was changed. When the bypass valve was 100 percent open, the pulsation near 2100 Hz was coincident with the mechanical natural frequency of the top turning vane. When the pulsation frequency was lowered from 2100 Hz to 1900 Hz, the strain levels on the top turning were significantly reduced because the pulsations were no longer coincident with the mechanical natural frequency near 2100 Hz.

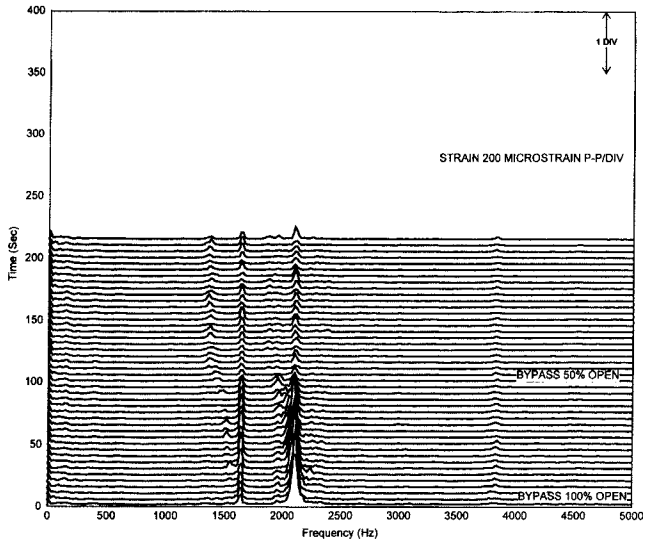

Figure 36. Strain on Upper Turning Vane as Bypass Valve Position Varied.

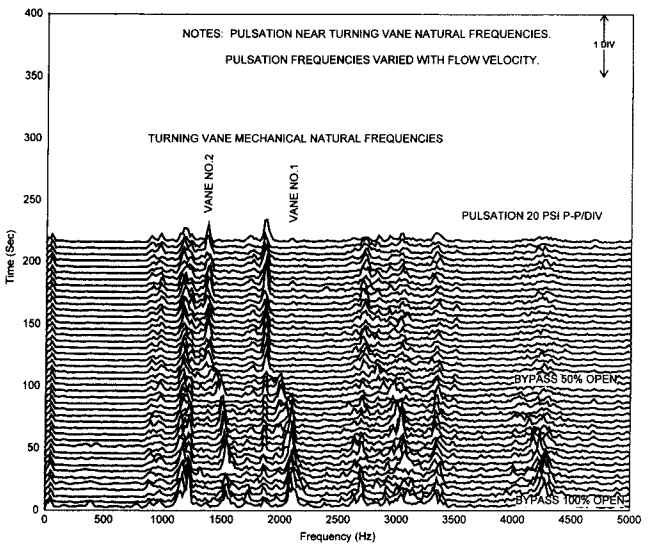

Figure 37. Pulsation Upstream of Turning Vane as Bypass Valve Position Varied.

Pulsation at a second acoustic natural frequency tracked from approximately 1600 Hz to 1400 Hz as the bypass valve was closed from 100 percent open to 50 percent open (Figure 37). When the pulsation frequency was reduced to approximately 1400 Hz, the pulsation energy was coincident with the mechanical natural frequency of the second turning vane and the strain levels were increased on the second turning vane (Figure 38). These data indicated that the turning vanes could be excited over a large range of operating conditions.

The acceleration frequencies measured on the second stage miter joint correlated with the strain frequencies measured on the turning vane. As shown in Figure 39, there were several major responses between 1000 Hz and 7000 Hz. The acceleration levels were generally reduced as the bypass valve was closed to 50 percent open. The good correlation indicated that the acceleration data measured on the miter joint could be used to determine if the vibration levels and resulting strain levels on the turning vanes would be excessive.

Acoustic Cross-Wall Natural Frequencies

The cross-wall acoustic natural frequencies for the first to second interstage piping were computed and compared with the measured pulsation responses in Table 10.

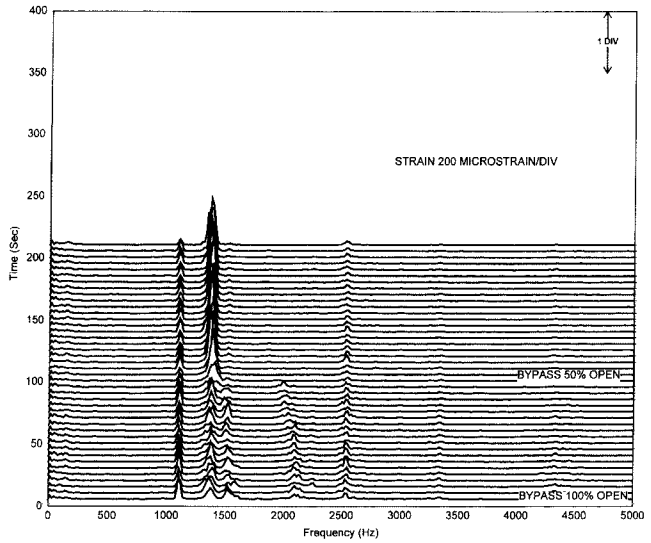

Figure 38. Strain on Second Turning Vane as Bypass Valve Position Varied.

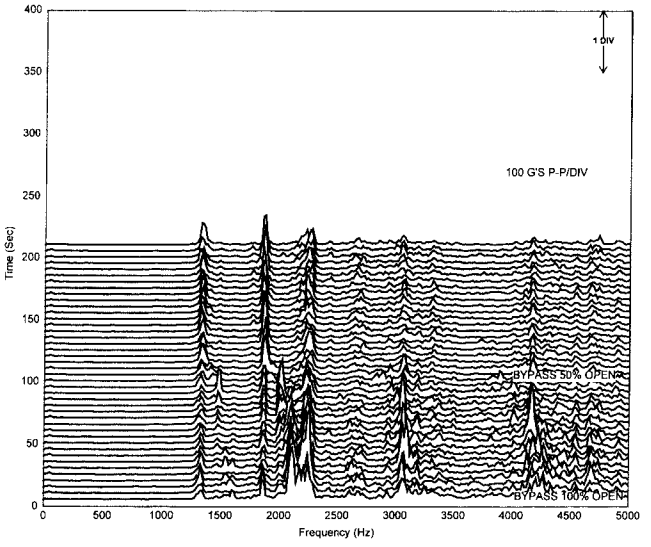

Figure 39. Acceleration on Miter Joint as Bypass Valve Position Varied.

Table 10. Comparison of Calculated and Measured Cross-Wall Acoustical Natural Frequencies.

First - Second Interstage (Pipe Diameter = 9.8 inch)		
(m, n)	Cross-Wall Acoustic Natural Frequencies (Hz)	
	Calculated	Measured
(1, 0)	907	900
(2, 0)	1504	1400
(0, 1)	1888	1850
(3, 0)	2071	2100
(1, 1)	2627	2700
(2, 1)	3307	3350
(1, 2)	4210	4250

The cross-wall natural frequencies are a function of the speed of sound, which for this case is primarily controlled by the temperature and the pressure of the nitrogen. The calculations were based upon a speed of sound of 1260 ft/sec.

As shown, there was excellent correlation between the calculated acoustic natural frequencies and the measured response frequencies. The pulsation data indicated that several of these cross-wall modes occurred simultaneously and were thought to be the primary cause for the excessive vibration and noise levels in the interstage piping. Several of these pulsation frequencies were also coincident with the mechanical natural frequencies of the turning vanes.

Modifications

One obvious modification to prevent the failures of the turning vanes was to remove the turning vanes. Therefore, it was recommended that the turning vanes should be removed and replaced with a flow splitter to direct the flow into the second stage impeller. In addition to directing the flow, the flow splitter would also break up the cross-wall modes. The miter joint was replaced with a long radius elbow and a flow splitter was installed as shown in Figure 40.

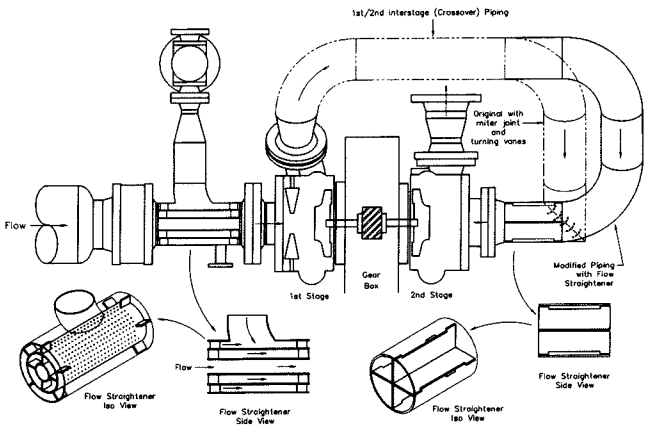

Figure 40. Modifications Installed to Prevent Formation of Cross-Wall Modes.

Although it was thought that these modifications would improve the flow into the second stage impeller, the pulsation in the interstage piping upstream of the flow splitter could still exist and could possibly cause fatigue failures of the flow splitter. It was felt that the required solution was to improve the flow into the IGVs. There were several possible modifications; however, it was felt that the most feasible modifications would be to install a second flow splitter just upstream of the IGVs. As shown in Figure 40, a flow splitter was designed which consisted of a 4 inch pipe mounted inside an 8 inch pipe. The flow from the bypass valve entered the flow splitter through perforations in the outer 8 inch pipe. The perforations were designed to also dampen the pulsations and reduce the turbulence from the bypass valve.

The new flow splitters were installed directly upstream of the first and second stage impellers. Since these flow splitters could possibly experience fatigues, it was decided to install strain gauges on both flow splitters. The strain data indicated that the vibration and strain levels on the splitters were low.

The inlet flow splitter reduced the pulsation in the first stage inlet piping upstream of the IGVs. Reducing the pulsation also reduced the strain levels on the IGVs. The pulsation levels at the midpoint of the first to second stage interstage piping were significantly reduced after the modifications were installed. The pulsation levels at the entrance to the second stage impeller were also reduced. The acceleration levels on the elbow at the second stage suction were also significantly reduced. After the modifications were installed, the vibrations on the interstage piping were low amplitude.

The compressor continued to operate satisfactorily after the modifications were installed. These modifications were later installed in another compressor at the site and both compressors continued to operate with no additional failures.

Steel Plant—Screw Compressors

The discharge silencers installed on screw compressors experienced fatigue failures after only a few hours of operation. Noise levels near the compressors were extremely high and the noise levels were still excessive outside the plant boundaries. Field tests and calculations showed that the excessive noise levels and the fatigue failures were due to coincidences of acoustic cross-wall natural frequencies and mechanical shell wall natural frequencies.

Instrumentation Problems Due to the High-Frequency Vibration

In an effort to determine the cause(s) for the fatigue failures of the silencers and the excessive noise levels, the plant personnel attempted to measure the vibration levels on the silencers. Initial vibration spectra indicated vibration levels of approximately 1000 mils peak-to-peak (1 inch peak-to-peak) at low frequencies less than 10 Hz. Although the plant personnel felt that the data were correct, it was unlikely that the compressor was actually vibrating with displacements of 1 inch peak-to-peak at any frequency. In addition, this high amplitude vibration should be easily visible.

It was later determined that these vibration data were indeed incorrect. The actual vibrations were not low-frequency vibration, but were high-frequency vibration above 1000 Hz with amplitudes greater than 500 g's zero-peak. Subjectively, the vibration was characterized by a "buzzing feel." Initially, a high sensitivity accelerometer (100 mv/g) had been used in an attempt to measure the high amplitude vibrations. The high-frequency accelerations caused the accelerometer amplifier to be overloaded, which resulted in a clipped signal (similar to a square wave). This clipped signal was then electronically double-integrated, which resulted in the high displacement amplitude at the low frequency. This illustrates the types of problems that can occur when measuring high amplitude, high-frequency accelerations.

The actual acceleration levels were later measured using a low sensitivity accelerometer (10 mv/g). Even with the low sensitivity accelerometers, it was difficult to measure the high amplitude, high-frequency accelerations. Initially, the accelerometers were mounted on pads that were epoxied to the pipe; however, the epoxy glue joint would fail within a few seconds after the compressor started. To eliminate the problems with the epoxy, the accelerometers were attached to steel pads that were welded to the pipe. The accelerometers remained attached to the piping, but the coaxial connectors on the accelerometers also failed after a few seconds. This connector failure problem was improved by soldering the wires to special adapters that were installed on the accelerometers. Also, it was determined that the quality of the coaxial connectors varied between manufacturers and that certain brands were able to withstand the high amplitude vibration without experiencing a failure.

The high vibration levels also caused similar problems with the pressure transducers. To avoid stub resonances, the pulsation data were obtained using insertion probes (refer to the section, *Insertion Probes*). The high-frequency vibration also caused fatigue failures of the coaxial connectors on the pressure transducers, and fretting problems on the stainless steel tubing of the insertion probes. In addition, one of the pressure taps experienced a fatigue failure that caused loss of both the tap and insertion probe. The failure did not result in a fire since the compressor was operating on nitrogen at that time. Although no one was injured when the tap broke away from the main pipe, this failure illustrates the potential dangers of conducting tests on piping with excessive high-frequency vibration levels.

Pulsation Generation in Screw Compressors

The dry screw compressor consists of a female rotor with six helical lobes and a male rotor with four helical lobes that intermesh with each other (Figure 41). The intermeshing of the helical lobes generate pulsation at the pocket-passing frequency that is equal to the number of lobes on the male rotor (four) multiplied by the compressor running speed. In addition to the pocket-passing frequency, pulsations are also generated at multiples of the pocket-passing frequency.

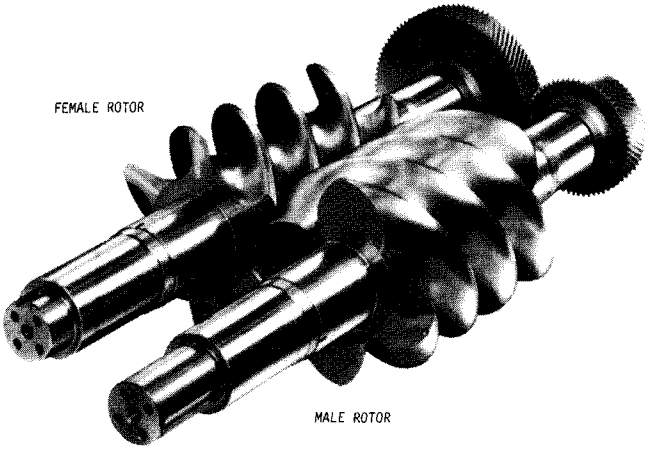

Figure 41. Dry Screw Compressor with Helical Rotors.

Normally, the maximum pulsation amplitudes occur at the fundamental pocket-passing frequency. Nordquist, et al. (1992), showed that the amplitude at the second pocket-passing frequency is normally one-half or one-third of the primary pocket-passing frequency amplitude. Normally, amplitudes at the higher multiples are even lower. However, the pulsation levels at the higher orders can be significantly amplified when the pulsations are coincident with the acoustic cross-wall natural frequencies.

Previous field tests on similar screw compressors have shown that significant pulsations up to the tenth harmonic of the pocket-passing frequency (40× running speed) can occur. These tests have also shown that most of the problems due to excessive pulsation, vibration, and noise occurred in the discharge piping. The pulsation levels are generally significantly lower on the suction side of the screw compressors, which was also the case with these compressors. Data obtained on the suction side of the compressors showed that the pulsation and vibration levels were low and that no modifications were required.

Screw compressors require silencers (pulsation filters) on both the inlet and discharge piping. These pulsation filters are theoretically designed to control the peak-to-peak pulsation levels to approximately 2 percent of the line pressure that is the level specified by API 619. An allowable sound pressure level of 90 dB measured 3 ft from the compressor is often specified by the user. However, most installations cannot meet this sound level and many screw compressors have to be installed inside sound enclosures. In addition, most of the pulsation filters are treated with sound insulation (glass fiber enclosed with an outer metal lagging) to attenuate the transmitted noise and the reradiated noise due to the shell wall vibration.

Typical pulsation filters consist of two or three chambers connected by smaller diameter choke tubes (Figure 42). These reactive filters are referred to as volume-choke-volume filters and are designed to attenuate the fundamental pocket-passing frequency. The choke tube lengths are usually sized to avoid acoustic natural frequencies (length resonances) of the choke tube, which are coincident with the higher multiples of the pocket-passing frequency. Similarly, lengths of the chambers are also sized to prevent acoustic natural frequencies of the pocket-passing frequencies.

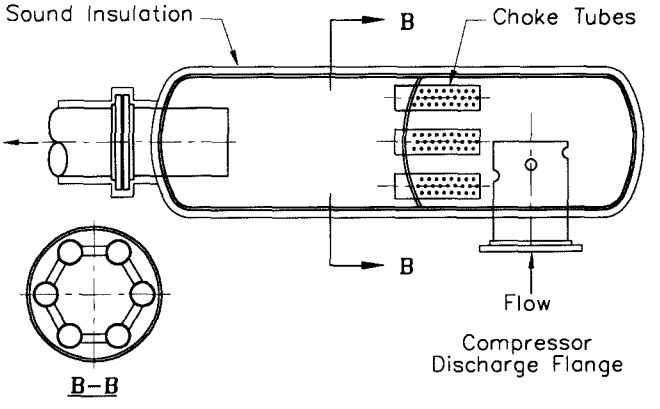

Figure 42. Typical Reactive Pulsation Filter.

Most of these volume-choke-volume pulsation filters are effective in attenuating the pulsation at the fundamental pocket-passing frequency. Pulsation data obtained on these screw compressors indicated that the transmitted pulsation level at the pocket-passing frequency was low.

However, these pulsation filters are generally not effective in attenuating the pulsation at the higher multiples of the pocket-passing frequency and can even amplify the energy at these frequencies. Most of these filters are designed assuming that the pulsations are plane waves where the length of the waves is much longer than the diameter of the pipe. However, at the higher multiples of the pocket-passing frequency, the wavelengths are small enough so that three-dimensional cross-wall modes can be excited.

These cross-wall natural frequencies can significantly amplify the pulsation levels generated by the compressor. Therefore, these silencers can attenuate the lower frequency pulsation while actually amplifying the higher frequency pulsation. The higher frequency pulsations are especially objectionable because the pulsation can propagate unattenuated for long distances down the piping. In addition, the high-frequency pulsation can excite the shell wall natural frequencies of the filter and the piping, which then results in excessive vibration, strain, and noise levels. This was the basic cause of the fatigue failures of the silencers.

There appears to be some confusion between some screw compressor manufacturers, silencer manufacturers, and end users regarding the design philosophies of the pulsation filters, and the allowable pulsation and noise levels. Some screw manufacturers state that the pulsation filters should not be referred to as silencers because this implies sound reduction. These manufacturers state that the pulsation filters are designed to only attenuate the pulsation at 1× and 2× pocket-passing frequency, and that the attenuation of the higher harmonics of the pocket-passing frequency is not a design goal. Some filter designers also agree with this philosophy, because it is difficult to attenuate the higher harmonics with a reactive silencer. Generally, the end user is not aware of these limitations in the design and expects the pulsation filters to attenuate all the pulsations, not just the pulsation at the first two harmonics of the pocket-passing frequency. As discussed, these filters often attenuate the pulsations at the fundamental pocket-passing frequency while amplifying the pulsation at the higher harmonics.

API 619 (1997) states: "*The primary function of silencers shall be to provide the maximum practical reduction of pulsations in the frequency range of audible sound without exceeding the specified pressure drop limit...unless otherwise agreed upon, the pressure drop through each silencer is limited to 1 percent of the absolute pressure at the silencer inlet.*"

Effects of Operating Conditions on Cross-Wall Natural Frequencies

The compressors were driven by electric motors at constant speeds. During the tests, the pulsation amplitudes of the various harmonics of the pocket-passing frequency varied as the discharge pressure was changed and when the gas composition was changed (Figure 43). Since the compressor running speed could not be varied, it was difficult to determine if the high pulsation levels at multiples of the pocket-passing frequency were amplified by the cross-wall natural frequencies.

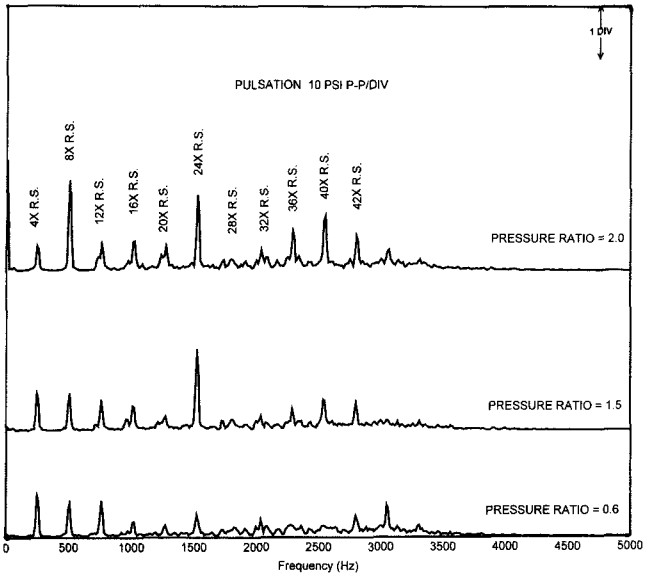

Figure 43. Screw Compressor Discharge Pulsation as Pressure Ratio Changed.

Calculations showed that these variations in the pulsation levels were due to changes in the speed of sound of the gas, which shifted the acoustic cross-wall natural frequencies. When the cross-wall natural frequencies shifted, some of the natural frequencies were coincident with the pocket-passing frequencies, and some of the other natural frequencies were no longer coincident. This resulted in amplification of pulsation at some of the multiples of the pocket-passing frequency and a reduction of pulsation at others.

The shifting of the acoustic natural frequencies caused a significant variation in the pulsation frequencies. This is important because it can explain why the compressors were sensitive to slight changes in the operating conditions (pressure, temperature, and gas composition). This can also explain why a compressor can operate satisfactorily with low pulsation, vibration, and noise levels in the shop, and then operate unsatisfactorily at the site with slightly different operating conditions.

Pulsation Reduction with High-Pressure Drop Orifice

It was recommended that the pulsation and the resulting vibration and strain levels be reduced by at least a factor of 10. The long-term solution would be to design and install silencers that would be effective in reducing the pulsation generated by the compressors without amplifying the higher harmonics of the pocket-passing frequency. A reactive silencer similar to that discussed in the following section could have been designed; however, due to time limitations, a reactive silencer was not an option.

The short-term solution was to install orifice plates with high-pressure drop at the compressor discharge flange. It was shown that orifice plates with high-pressure drops of 10 percent to 40 percent of the discharge line pressure reduced the discharge pulsation to acceptable levels. Although this high-pressure drop was effective in attenuating the high-frequency pulsation, the high-pressure drop significantly increased the load on the motors and increased the power costs. Although the operating costs were increased, the motors had excess capacity, which allowed the compressors to operate with the high-pressure drop. The plant felt that this would be acceptable until a long-term solution could be installed.

Refinery—Screw Compressor

The discharge system for a screw compressor in a refinery service was experiencing failures of piping, silencer internals, and instrumentation. Noise levels were also high in the vicinity of the compressor. After several unsuccessful efforts at reducing the vibration and noise, a project to create a new silencer design was begun.

The vibration and failures were thought to be due to acoustic cross-wall mode formation in the silencer. However, because of the service, it was not possible to design an absorptive silencer. Therefore, the design had to incorporate elements that would provide reactive filtering, but not introduce the high-order acoustical modes.

Based upon previous experience, it was determined that it was impractical to use three-dimensional computational methods to develop an improved silencer design. Therefore, the design used traditional one-dimensional reactive silencer design principles, but in a new way. Instead of providing a single large silencer, the new design was essentially many smaller parallel silencers. This philosophy resulted in silencer dimensions that were small enough so that the lowest cross-wall acoustic modes were above 10× the primary excitation frequencies, while the multiple paths limited pressure drop through the silencer to acceptable levels. A schematic of the silencer is shown in Figure 44. Note in the cross-section that many parallel paths were constructed in a single shell.

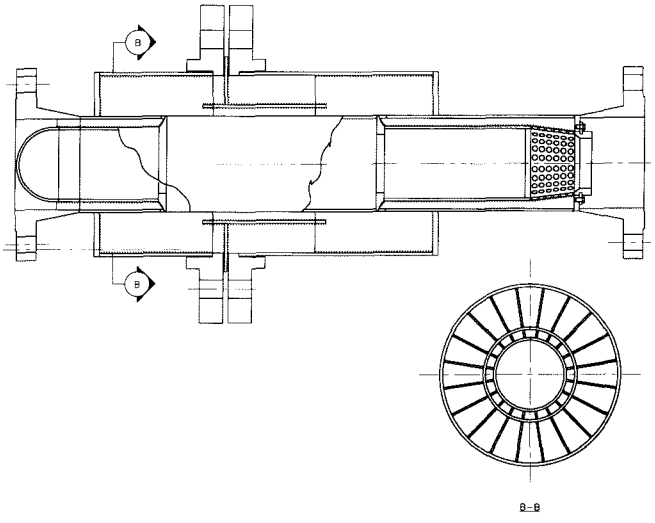

Figure 44. High-Frequency Reactive Silencer Schematic.

The silencer was constructed and installed. Figure 45 shows one step of the construction process. After installation of the new silencer, plant personnel reported dramatic reductions in piping vibration. The compressor has been operating for a number of years without piping failures.

Variations of this silencer design have also been tried with success. It should be noted that compared with off-the-shelf silencers, this design is significantly more expensive to design and fabricate. However,the improved reliability justifies the additional cost in critical applications.

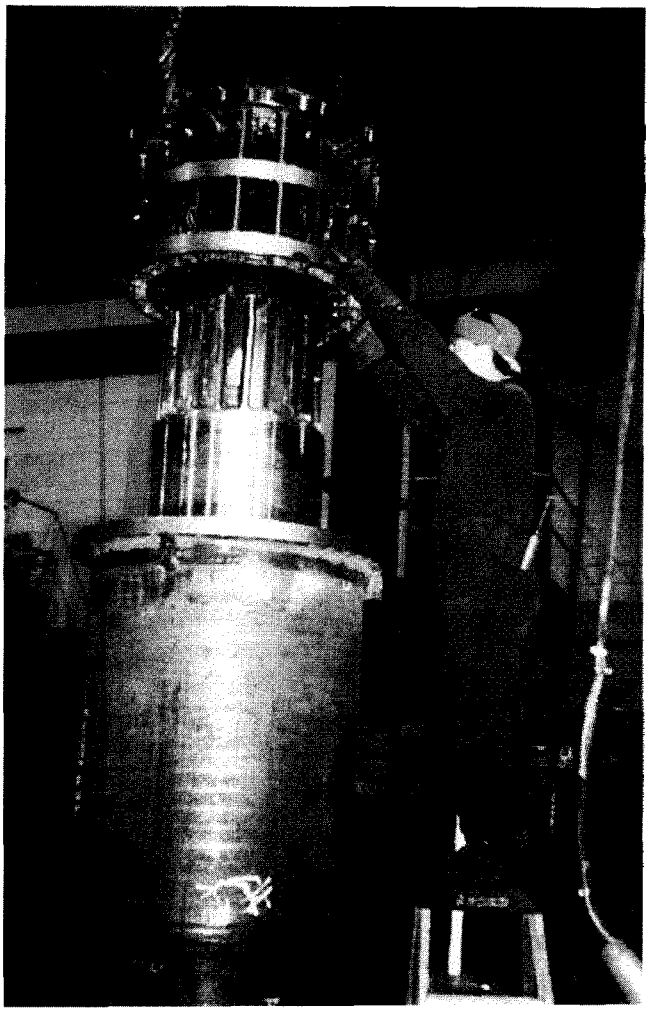

Figure 45. Fabrication of High-Frequency Silencer.

SUMMARY

The fundamentals governing the generation of high-frequency energy by excitation of high-order acoustical modes and shell wall natural frequencies have been presented. Using the equations provided, spreadsheet applications can be generated to determine the potential for problems in a system.

Methods for instrumentation and test of installed systems have also been presented. Using the techniques provided, the reader should be able to recognize and diagnose these types of problems when they occur.

Devices for preventing formation of high-order acoustical modes and methods to attenuate the energy have also been discussed. Using "flow-splitters" and "tube-bundles" was shown to be effective, although more research needs to be conducted to determine the exact dimensions required. A high-frequency *reactive silencer design* has also been shown to be effective in preventing the formation of higher order acoustical modes.

Finally, the case histories provided several instances where the techniques were used to solve problems in the field. These studies were selected to illustrate the range of problems that can be encountered that have essentially the same underlying causes.

REFERENCES

API Standard 619, 1997, "Rotary Type Positive Displacement Compressors for General Refinery Service," American Petroleum Institute, New York, New York.

Blevins, R. D., 1973, *Flow Induced Vibration*, New York, New York: Van Nostrand Reinhold Company.

Blevins, R. D., 1979, *Formulas for Natural Frequency and Mode Shape*, New York, New York: Van Nostrand Reinhold Company.

Kinsler, L. E., Frey, A. R., Coppens, A. B., and Sanders, J. V., 1982, *Fundamentals of Acoustics*, Third Edition, New York, New York: John Wiley & Sons, pp. 167-169.

Mikasinovic, M., 1989, "Vibration Acceptance Criteria of Circular Cylinder Shells," *Pipeline Dynamics and Valves-1989*, ASME PVP, 180, pp. 47-52.

Nordquist, G. B., Bielskus, P. A., and Clayton, R., 1992, "Dry Screw Compressors in Process Applications Including Maintenance Considerations," *Proceedings of the Twenty-First Turbomachinery Symposium*, Turbomachinery Laboratory, Texas A&M University, College Station, Texas, pp. 3-20.

Pelton, H. K., 1993, *Noise Control Management*, New York, New York: Van Nostrand Reinhold Company, pp. 152.

ACKNOWLEDGEMENTS

The authors wish to acknowledge the contributions of EDI staff members Jim Tison, Kile Watson, and Mark Broom for their assistance in the preparation of this paper.